

Cognitive Radio-Enabled Network-Based Cooperation: From a Connectivity Perspective

Weng Chon Ao and Kwang-Cheng Chen, *Fellow, IEEE*

Abstract—Cognitive radio (CR) enables dynamic spectrum access to provide universal connectivity across different types of radio access technologies, realizing seamless content delivery in the next generation wireless networking. As the most general cognitive radio network scenario, multiple ad hoc and infrastructure networks sharing the same spectrum are allowed to cooperate with each other by using other networks' nodes as relays to carry and forward traffic, forming an interconnected heterogeneous network. Previous research is limited to the connectivity analysis of hybrid wireless networks with path loss channel model. In this paper, we analyze the connectivity of the interconnected heterogeneous network consisting of multiple ad hoc networks and multiple infrastructure networks from a percolation-based perspective, considering both noise-limited and interference-limited environment with general fading channel model. The benefit of network-based cooperation is quantified in terms of the percolation threshold, facilitating proper network control and deployment. For example, using such quantification, we can specify the amount of infrastructure deployment or reliable connections to control the connectivity of existing ad hoc networks, and vice versa. Finally, we apply the analysis to the coexistence of primary and secondary networks, as the common CR scenario.

Index Terms—cooperative communications, connectivity, cognitive radio, ad hoc networks, infrastructure networks, heterogeneous networks, spectrum sharing

I. INTRODUCTION

COGNITIVE radio (CR) technologies [1], [2] enable dynamic spectrum access such that intercommunication (interconnection or internetworking) among different types of networks becomes feasible, facilitating universal connectivity and seamless content delivery. In this paper, we consider the most general cognitive radio network (CRN) scenario, to have several heterogeneous wireless networks cooperatively form a general ad hoc network by sharing the same spectrum, as was raised in [3] and likely for large spectrum sharing sensor networks or machine-to-machine communications. Part of a wireless network may have wired/wireless infrastructure. Furthermore, one or some wireless networks may have priority in utilizing this spectrum (as the primary systems in common CR scenario).

In this general CRN, different types of networks, including infrastructure-based networks and infrastructure-less networks,

Manuscript received 5 January 2012; revised 16 May 2012. This work was supported by the National Science Council and INTEL Corp. under the Contract NSC 100-2911-I-002-001.

W. C. Ao is with the Department of Electrical Engineering, University of Southern California, Los Angeles, CA 90089 USA (e-mail: wao@usc.edu).

K.-C. Chen is with the Graduate Institute of Communication Engineering, National Taiwan University, Taipei 10617, Taiwan (e-mail: chenkc@cc.ee.ntu.edu.tw).

Digital Object Identifier 10.1109/JSAC.2012.121112.

cooperate with each other (termed network-based cooperation) to carry and forward data traffic. Nodes in infrastructure-based networks are often connected with wired (or reliable wireless) backbone, e.g., nodes in smart grids are connected with power line and base stations in cellular networks are connected with wired backhaul; while nodes in infrastructure-less networks (e.g., mobile ad hoc networks and sensor networks) are connected with wireless radio broadcasting. For example, with network-based cooperation as shown in Fig. 1, a packet generated by a node in ad hoc network \mathcal{A}_1 may be relayed (by nodes in \mathcal{A}_1 and/or \mathcal{A}_2) in single-hop/multi-hop fashion to a base station in infrastructure network \mathcal{B}_1 , and then forwarded via backhaul to another base station in the infrastructure network, and finally delivered to another node in ad hoc network \mathcal{A}_1 in a single-hop/multi-hop fashion.

It is important to understand the capacity and connectivity of a network so that proper network operations can be performed. While there exists a significant amount of literature on the capacity scaling laws of homogeneous wireless ad hoc networks [4] and hybrid (cellular ad hoc) wireless networks [5]–[7], in this paper we focus on the connectivity analysis useful for networking algorithms. It appears to be intuitive that connectivity can be improved with network-based cooperation, under which different types of networks cooperate with each other by using other networks' nodes as relays to forward traffic. However, it is much harder to understand to what extent the network connectivity can be improved, and to quantify the benefit of network-based cooperation.

Connectivity of a homogeneous wireless ad hoc network has been received much attention. 1-connectivity and k -connectivity of a network were studied in [8] and [9], respectively. On the other hand, in many applications such as mobile ad hoc networks and sensor networks, 1-connectivity is difficult to be maintained and is not required. A weaker connectivity from a percolation-based perspective (i.e., a nonvanishing fraction of nodes in the network, say, 90%, are connected) is more appropriate. For example, significant savings in power consumption may be achieved by allowing a small fraction (say, 10%) of nodes to be disconnected [10], [11]. For an infinite network with density λ and transmission range r (i.e., a random geometric network [12]), the network percolates, in which an infinite connected component appears, when the mean degree of a network node is above a threshold (i.e., $\lambda\pi r^2 \geq 4.52$). Otherwise, the network does not percolate and will be partitioned into many isolated finite clusters. In [11], [13], the impact of channel fading on the percolation threshold of an ad hoc network was investigated, and its effect on the mean degree of a network node was discussed in [14],

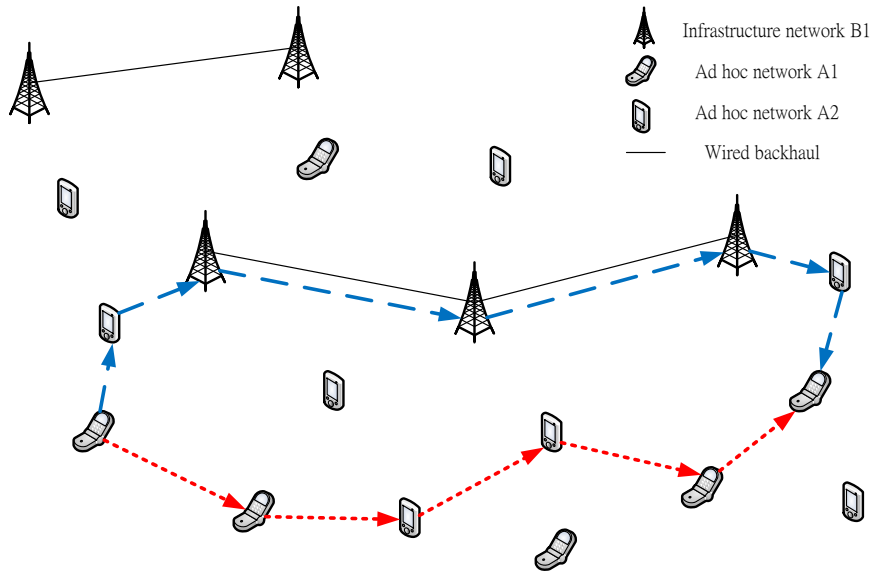


Fig. 1. With network-based cooperation, a packet generated by a node in ad hoc network \mathcal{A}_1 may be relayed (by nodes in \mathcal{A}_1 and/or \mathcal{A}_2) in single-hop/multi-hop fashion to a base station in infrastructure network \mathcal{B}_1 , and then forwarded via backhaul to another base station in \mathcal{B}_1 , and finally delivered to another node in \mathcal{A}_1 in a single-hop/multi-hop fashion. Red arrows and blue arrows indicate two paths of packet flows, respectively.

[15]. Dousse *et al.* [16] studied percolation in an ad hoc network with self co-channel interference. In [17], connectivity of a network with unreliable links was analyzed in a percolation sense. Percolation of an ad hoc network employing physical layer cooperative techniques was addressed in [18], in which nodes may form a group to perform distributed beamforming so that signals are coherently combined at some distant destinations.

However, limited attention has been drawn on the connectivity analysis of an interconnected heterogeneous network with network-based cooperation. Dousse *et al.* [19] used percolation theory to analyze the connectivity of hybrid wireless networks in which base stations act as relay nodes for routing and forwarding packets from/to nodes in an ad hoc network. They computed the probability that an arbitrary node is connected to a base station under disk model without considering fading and interference. The isolation probability that an ad hoc node cannot be connected to a base station in single-hop was further computed in [20] considering Rayleigh fading channel model and cochannel interference. Under a similar network model as in [19], Yi *et al.* [21] found that when the density of base stations λ_β satisfies $0 < \lambda_\beta < c_1(\lambda_\alpha)^1$ and the base stations as well as ad hoc nodes have the same transmission range, the number of connected ad hoc nodes is $\Theta(n)$ and scales linearly with λ_β . Percolation of the ad hoc network is facilitated by the deployment of base stations. Connectivity of a common CRN consisting of primary and secondary ad hoc networks was studied in [22]–[24]. For example, in [22], the connectivity of the secondary network is parameterized by the tuple $(\lambda_{PT}, \lambda_{SU})$ under path loss channel model, where λ_{PT} is the density of primary transmitters and λ_{SU} is the density of secondary users. The secondary network percolates only when λ_{PT} is below some threshold and λ_{SU} is above some threshold. In [24], cooperation is further considered

among secondary ad hoc networks. In spite of the above efforts, there lacks a framework to analyze the connectivity of a general CRN, an interconnected heterogeneous network consisting of multiple ad hoc and infrastructure networks with general fading channels.

In this paper, we analyze the connectivity of an interconnected heterogeneous network from a percolation-based perspective, in which different types of networks cooperate with each other by using other networks' nodes as relays to carry and forward data traffic. To our knowledge, it is the first framework to consider the effects of network-based cooperation (among multiple ad hoc networks and multiple infrastructure networks) on the network connectivity, in both noise-limited and interference-limited environment with general fading. The benefit of network-based cooperation is characterized in terms of the percolation threshold, allowing understanding of macroscopic network behavior that is fundamentally different from traditional microscopic investigations on a single link or interaction among several links (e.g., the diversity gain for a source-destination pair with multiple cooperative relays). Quantification of connectivity improvement facilitates network control and deployment. For example, with such quantification, we can compute the amount of infrastructure to be deployed to improve the connectivity of an existing ad hoc network, and vice versa. Also, when there exist multiple ad hoc networks in a noise-limited environment, to maintain a certain mean degree (connectivity), we can reduce transmit power of each individual network with network-based cooperation. While in an interference-limited environment, to maintain a certain mean degree, the access probability (capacity) of each network can be increased with network-based cooperation.

The contributions and the role of CR in this paper are summarized as follows.

¹The value $c_1(\lambda_\alpha)$ depends on the ad hoc node density λ_α , where λ_α is supposed to be smaller than the percolation threshold.

- 1) We derive the mean degree and the degree distribution of a network node in both noise-limited and interference-

TABLE I
MAIN NOTATIONS

Description	Notation		
	Ad hoc networks $\mathcal{A}_i, 1 \leq i \leq M$	Infrastructure networks $\mathcal{B}_i, 1 \leq i \leq N$	Interfering networks $\mathcal{C}_i, 1 \leq i \leq S$
Node density	$\lambda_{\mathcal{A}_i}$	$\lambda_{\mathcal{B}_i}$	$\lambda_{\mathcal{C}_i}$
The set of locations of nodes	$\Phi_{\mathcal{A}_i}$	$\Phi_{\mathcal{B}_i}$	$\Phi_{\mathcal{C}_i}$
Transmit power	$P_{\mathcal{A}_i}$	$P_{\mathcal{B}_i}$	$P_{\mathcal{C}_i}$
Information rate	$R_{\mathcal{A}_i}$	$R_{\mathcal{B}_i}$	$R_{\mathcal{C}_i}$
Fading gain	$G_{x,y}, x, y \in \{\mathcal{A}_i, \mathcal{B}_i, \mathcal{C}_i\}$		
Inverse Laplace transform of cdf of $G_{x,y}$	$g_{x,y}(t), x, y \in \{\mathcal{A}_i, \mathcal{B}_i\}$		
Degree distribution	$p_{\mathcal{A}_i}(k)$	$p_{\mathcal{B}_i}(k)$	
Mean degree (noise-limited)	$\beta_{x,y}, x, y \in \{\mathcal{A}_i, \mathcal{B}_i\}$		
Mean degree (interference-limited)	$\beta_{x,y}, x, y \in \{\mathcal{A}_i, \mathcal{B}_i\}$		
Medium access probability	$p_{\mathcal{A}_i}$	$p_{\mathcal{B}_i}$	
The set of locations of transmitters	$\Phi_{\mathcal{A}_i}^1$	$\Phi_{\mathcal{B}_i}^1$	
The set of locations of receivers	$\Phi_{\mathcal{A}_i}^0$	$\Phi_{\mathcal{B}_i}^0$	
Transmitter-receiver distance			d_i
Outage probability constraint			ϵ_i
Path loss exponent	$\alpha, \delta = 2/\alpha$		
Background noise power	N_0		

limited environment with general fading channel model.

- 2) Based on 1), we analyze the necessary condition for percolation of cooperative ad hoc networks and infrastructure networks sharing the same spectrum, as the most general CRN scenario. Dedicated communication links in the infrastructure may therefore act as a mean to control the overall network connectivity.
- 3) Based on 2), we apply the analysis to study the connectivity of cooperative secondary (unlicensed) networks coexisting with primary (licensed) networks. The secondary networks sustain interference from primary transmitters, whereas the access probabilities of secondary network nodes are restricted due to outage probability constraints at primary receivers, as well-known definition of CRN.

The remainder of this paper is organized as follows. In Section II, we analyze the network connectivity with cooperation among multiple ad hoc networks and multiple infrastructure networks in a noise-limited environment. In Section III, we generalize the results to the interference-limited case. Coexistence of primary and secondary networks is addressed in Section IV. Numerical results are provided in Section V. Section VI gives the conclusion.

II. NOISE-LIMITED ENVIRONMENT

In the first two subsections, we study the percolation threshold of an ad hoc network and an infrastructure network. In the last three subsections, we study the percolation condition of cooperative ad hoc networks, cooperative infrastructure networks, and a heterogeneous network with cooperation among both ad hoc networks and infrastructure networks. The main notations are summarized in Table I.

A. Wireless ad hoc networks

In this subsection, we successively derive the mean degree, the degree distribution, and the percolation threshold of an ad hoc network. We consider M wireless ad hoc networks (denoted as $\mathcal{A}_i, 1 \leq i \leq M$). In \mathcal{A}_i , the spatial distribution of nodes is assumed to follow a homogeneous Poisson point process (PPP) with density $\lambda_{\mathcal{A}_i}$. Let $\Phi_{\mathcal{A}_i} = \{X_k^{\mathcal{A}_i}\}$ denote the set of locations of the nodes and let $P_{\mathcal{A}_i}$ denote the transmit power of a node. The information rate of a node is assumed to be $R_{\mathcal{A}_i}$ and the fading gains between any pair of nodes in \mathcal{A}_i are supposed to be independently drawn according to some distribution $f_{G_{\mathcal{A}_i, \mathcal{A}_i}}(x)$. A pair of nodes in \mathcal{A}_i are connected (i.e., there exists a link between them and they are considered as one-hop neighbors of each other) if the capacity of the channel between them can support the information rate $R_{\mathcal{A}_i}$, i.e., $\log\left(1 + \frac{G_{\mathcal{A}_i, \mathcal{A}_i} P_{\mathcal{A}_i} r^{-\alpha}}{N_0}\right) \geq R_{\mathcal{A}_i}$, where r is the distance between the pair of nodes, α is the path loss exponent, and N_0 is the background noise power.

Consequently, one-hop neighbors of the typical node of \mathcal{A}_i (a reference node located at the origin)² are resulted from independent thinning of each node $x \in \Phi_{\mathcal{A}_i}$ with probability $\mathbb{P}\left(\log\left(1 + \frac{G_{\mathcal{A}_i, \mathcal{A}_i} P_{\mathcal{A}_i} \|x\|^{-\alpha}}{N_0}\right) \geq R_{\mathcal{A}_i}\right)$. $\|x\|$ denotes the distance between the typical node and the node at x . By the mapping theorem [26], the number of one-hop neighbors (or the degree) of the typical node of \mathcal{A}_i is Poisson distributed with mean $\beta_{\mathcal{A}_i, \mathcal{A}_i}$, which can be computed as

²By the stationarity of homogeneous PPP [25], the statistics measured by the typical node is representative for all other nodes. Therefore, we focus our discussions on the typical node. A typical node may be a transmitter or a receiver depending on the context.

$$\begin{aligned}
\beta_{\mathcal{A}_i, \mathcal{A}_i} &= \int_0^\infty \lambda_{\mathcal{A}_i} \\
&\times \mathbb{P}_{G_{\mathcal{A}_i, \mathcal{A}_i}} \left(\log \left(1 + \frac{G_{\mathcal{A}_i, \mathcal{A}_i} P_{\mathcal{A}_i} r^{-\alpha}}{N_0} \right) \geq R_{\mathcal{A}_i} \right) 2\pi r dr \\
&= \mathbb{E}_{G_{\mathcal{A}_i, \mathcal{A}_i}} \left[\int_0^\infty \lambda_{\mathcal{A}_i} \mathbf{1} \left(r \leq \left(\frac{G_{\mathcal{A}_i, \mathcal{A}_i} P_{\mathcal{A}_i}}{(2^{R_{\mathcal{A}_i}} - 1) N_0} \right)^{\frac{1}{\alpha}} \right) 2\pi r dr \right] \\
&= \mathbb{E}_{G_{\mathcal{A}_i, \mathcal{A}_i}} \left[\lambda_{\mathcal{A}_i} \pi \left(\frac{G_{\mathcal{A}_i, \mathcal{A}_i} P_{\mathcal{A}_i}}{(2^{R_{\mathcal{A}_i}} - 1) N_0} \right)^\delta \right] \\
&= \frac{\lambda_{\mathcal{A}_i} \pi P_{\mathcal{A}_i}^\delta \mathbb{E}[G_{\mathcal{A}_i, \mathcal{A}_i}^\delta]}{(2^{R_{\mathcal{A}_i}} - 1)^\delta N_0^\delta}, \tag{1}
\end{aligned}$$

where $\mathbf{1}(\cdot)$ is the indicator function, and $\delta = \frac{2}{\alpha}$. The probability that a node in \mathcal{A}_i has k one-hop neighbors (or degree k) is denoted as $p_{\mathcal{A}_i}(k)$, which satisfies

$$p_{\mathcal{A}_i}(k) = \frac{\exp(-\beta_{\mathcal{A}_i, \mathcal{A}_i}) \beta_{\mathcal{A}_i, \mathcal{A}_i}^k}{k!}, \quad k = 0, 1, 2, \dots \tag{2}$$

In conclusion, the degree distribution of wireless ad hoc network \mathcal{A}_i in a noise-limited environment is $p_{\mathcal{A}_i}(k)$, which is a Poisson distribution with mean degree $\beta_{\mathcal{A}_i, \mathcal{A}_i}$.

The concept of percolation originates from statistical physics and random networks [12], [27]. From (1), as the transmit power $P_{\mathcal{A}_i}$ increases, the mean degree $\beta_{\mathcal{A}_i, \mathcal{A}_i}$ increases. If we draw links between each node and its one-hop neighbors, the resulting network graph percolates and an infinite connected component appears in the network (called supercritical phase) when $\beta_{\mathcal{A}_i, \mathcal{A}_i}$ is above the percolation threshold $\beta_{\mathcal{A}_i, \mathcal{A}_i}^c$. On the other hand, when $\beta_{\mathcal{A}_i, \mathcal{A}_i}$ is below the percolation threshold, the network does not percolate and consists of many isolated finite components (called subcritical phase). The percolation threshold $\beta_{\mathcal{A}_i, \mathcal{A}_i}^c$ can be computed by finding the critical point at which the mean component size blows up, indicating the formation of an infinite connected component in the network. We describe the procedure of computing the percolation threshold in the following proposition.

Proposition 1. *The necessary condition for percolation of the ad hoc network \mathcal{A}_i is*

$$1 - \frac{\sum_{k=0}^{\infty} [k^2 - k] p_{\mathcal{A}_i}(k)}{\sum_{k=0}^{\infty} k p_{\mathcal{A}_i}(k)} = 1 - \beta_{\mathcal{A}_i, \mathcal{A}_i} = 0. \tag{3}$$

In other words, the lower bound on the percolation threshold is one. That is, if the ad hoc network \mathcal{A}_i percolates, the mean degree $\beta_{\mathcal{A}_i, \mathcal{A}_i}$ is greater than one.

Proof: The proof is presented in Appendix A. \blacksquare

Since we ignore the spatial dependency (i.e., two of a node's one-hop neighbors are likely one-hop neighbors themselves) in the computation, (3) serves as a necessary condition. It is known that in the case without fading, the network graph becomes the so-called random geometric graph with percolation threshold about 4.52. Channel fading produces spread-out connections and weakens the spatial dependency, and therefore reduces the percolation threshold [28]. The actual percolation threshold would be located between 1 and 4.52, depending on the fading distribution. The randomness due to fading and node mobility [13] could drive the percolation threshold down to 1.

B. Infrastructure networks

In this subsection, we successively derive the degree distribution and the percolation threshold of an infrastructure network. We consider N infrastructure networks (denoted as \mathcal{B}_i , $1 \leq i \leq N$). Nodes in infrastructure network \mathcal{B}_i (e.g., base stations or relay stations in cellular networks) are supposed to be connected by wired backhaul. Backhaul connections may even be established among nodes separated by long distances. The spatial distribution of nodes in \mathcal{B}_i is assumed to follow a PPP with density $\lambda_{\mathcal{B}_i}$.³ Let $\Phi_{\mathcal{B}_i} = \{X_k^{\mathcal{B}_i}\}$ denote the set of locations of the nodes. The nodes that have direct backhaul connections to the typical node of \mathcal{B}_i are referred to as the one-hop neighbors of the typical node. The probability that the typical node has k one-hop neighbors (or degree k) is denoted as $p_{\mathcal{B}_i}(k)$, which may follow a truncated geometric distribution with parameter p and threshold k_{\max} (i.e., $p_{\mathcal{B}_i}(k) = \frac{(1-p)^k p}{\sum_{j=0}^{k_{\max}} (1-p)^j p}$, $k = 0, 1, 2, \dots, k_{\max}$) [30]. The infrastructure network \mathcal{B}_i percolates when

$$1 - \frac{\sum_{k=0}^{\infty} [k^2 - k] p_{\mathcal{B}_i}(k)}{\sum_{k=0}^{\infty} k p_{\mathcal{B}_i}(k)} = 0. \tag{4}$$

C. Cooperation among multiple wireless ad hoc networks

In this subsection, we successively derive the degree distribution and the percolation condition of the cooperative ad hoc networks. Due to the broadcast nature of wireless communications, when a node in \mathcal{A}_i transmits a message, all nodes in \mathcal{A}_j , $1 \leq j \leq M$, could be potential receivers. If M wireless ad hoc networks cooperate with each other by carrying and forwarding each other's traffic, network connectivity can be improved. For example, messages from a node in \mathcal{A}_i may reach another node in \mathcal{A}_i in a multi-hop fashion, where intermediate hops may consist of nodes from \mathcal{A}_j , $1 \leq j \leq M$. With cooperation among M ad hoc networks, the degree distribution of a node in \mathcal{A}_i becomes

$$\begin{aligned}
p_{\mathcal{A}_i}(k_1, k_2, \dots, k_M) &= \frac{\exp(-\beta_{\mathcal{A}_i, \mathcal{A}_1}) \beta_{\mathcal{A}_i, \mathcal{A}_1}^{k_1}}{k_1!} \dots \frac{\exp(-\beta_{\mathcal{A}_i, \mathcal{A}_M}) \beta_{\mathcal{A}_i, \mathcal{A}_M}^{k_M}}{k_M!} \\
&= \exp \left(- \sum_{j=1}^M \beta_{\mathcal{A}_i, \mathcal{A}_j} \right) \prod_{j=1}^M \frac{\beta_{\mathcal{A}_i, \mathcal{A}_j}^{k_j}}{k_j!}, \\
&\quad k_j = 0, 1, 2, \dots, 1 \leq j \leq M, \tag{5}
\end{aligned}$$

where $\beta_{\mathcal{A}_i, \mathcal{A}_j}$ is the average number of nodes in \mathcal{A}_j that are one-hop neighbors of the typical node of \mathcal{A}_i . In other words, $\beta_{\mathcal{A}_i, \mathcal{A}_j}$ is the mean number of nodes in \mathcal{A}_j that can successfully decode the messages from the typical node of \mathcal{A}_i , being potential relays to carry and forward data traffic for \mathcal{A}_i .

³In [29], the spatial distribution of base stations following PPP is justified to be a good approximation.

$\beta_{\mathcal{A}_i, \mathcal{A}_j}$ can be computed as

$$\begin{aligned} \beta_{\mathcal{A}_i, \mathcal{A}_j} &= \int_0^\infty \lambda_{\mathcal{A}_j} \\ &\quad \times \mathbb{P}_{G_{\mathcal{A}_i, \mathcal{A}_j}} \left(\log \left(1 + \frac{G_{\mathcal{A}_i, \mathcal{A}_j} P_{\mathcal{A}_i} r^{-\alpha}}{N_0} \right) \geq R_{\mathcal{A}_i} \right) 2\pi r dr \\ &= \frac{\lambda_{\mathcal{A}_j} \pi P_{\mathcal{A}_i}^\delta \mathbb{E}[G_{\mathcal{A}_i, \mathcal{A}_j}^\delta]}{(2^{R_{\mathcal{A}_i}} - 1)^\delta N_0^\delta}, \end{aligned} \quad (6)$$

where the fading gains between any pair of nodes in \mathcal{A}_i and \mathcal{A}_j are supposed to be independently drawn according to some distribution $f_{G_{\mathcal{A}_i, \mathcal{A}_j}}(x)$.

We have the following proposition.

Proposition 2. *The necessary condition for percolation of the M cooperative ad hoc networks is*

$$\begin{vmatrix} 1 - \beta_{\mathcal{A}_1, \mathcal{A}_1} & -\beta_{\mathcal{A}_1, \mathcal{A}_2} & \cdots & -\beta_{\mathcal{A}_1, \mathcal{A}_M} \\ -\beta_{\mathcal{A}_2, \mathcal{A}_1} & 1 - \beta_{\mathcal{A}_2, \mathcal{A}_2} & \cdots & -\beta_{\mathcal{A}_2, \mathcal{A}_M} \\ \vdots & \vdots & \ddots & \vdots \\ -\beta_{\mathcal{A}_M, \mathcal{A}_1} & -\beta_{\mathcal{A}_M, \mathcal{A}_2} & \cdots & 1 - \beta_{\mathcal{A}_M, \mathcal{A}_M} \end{vmatrix} = 0, \quad (7)$$

where $|\cdot|$ denotes determinant. For all $i = 1, \dots, M$, the mean component size in \mathcal{A}_i reachable from a randomly selected node of \mathcal{A}_i (by potentially using other networks' nodes as relays) blows up when the determinant reaches its first zero.

Proof: The proof is presented in Appendix B. \blacksquare

When without cooperation among the ad hoc networks, all the off-diagonal entries are zero. (7) decomposes and reduces to (3). The benefit of cooperation comes from the introduction of off-diagonal entries, indicating that a message is able to circulate among different networks.

D. Cooperation among multiple infrastructure networks

In this subsection, we successively derive the degree distribution and the percolation condition of the cooperative infrastructure networks. Since nodes in infrastructure networks are often equipped with wireless transceivers (e.g., base stations and relay stations), packets originated from a node in an infrastructure network may be forwarded via its wired backhaul connections as well as wireless radio broadcasting. In the latter case, packets may be captured by nodes in other infrastructure networks. With cooperation among N infrastructure networks, the degree distribution of a node in \mathcal{B}_i becomes

$$\begin{aligned} p_{\mathcal{B}_i}(l_1, l_2, \dots, l_N) \\ = p_{\mathcal{B}_i}(l_i) \exp \left(- \sum_{j'=1, j' \neq i}^N \beta_{\mathcal{B}_i, \mathcal{B}_{j'}} \right) \prod_{j'=1, j' \neq i}^N \frac{\beta_{\mathcal{B}_i, \mathcal{B}_{j'}}^{l_{j'}}}{l_{j'}!}, \\ l_{j'} = 0, 1, 2, \dots, 1 \leq j' \leq N, \end{aligned} \quad (8)$$

where $p_{\mathcal{B}_i}(l_i)$ is defined in Section II-B as the degree distribution of wired backhaul connections in \mathcal{B}_i , and $\beta_{\mathcal{B}_i, \mathcal{B}_{j'}}$ is the average number of nodes in $\mathcal{B}_{j'}$ that can successfully decode the messages via radio broadcasting from the typical node of \mathcal{B}_i . $\beta_{\mathcal{B}_i, \mathcal{B}_{j'}}$ can be computed as

$$\beta_{\mathcal{B}_i, \mathcal{B}_{j'}} = \frac{\lambda_{\mathcal{B}_{j'}} \pi P_{\mathcal{B}_i}^\delta \mathbb{E}[G_{\mathcal{B}_i, \mathcal{B}_{j'}}^\delta]}{(2^{R_{\mathcal{B}_i}} - 1)^\delta N_0^\delta}, \quad (9)$$

where $P_{\mathcal{B}_i}$ and $R_{\mathcal{B}_i}$ are the transmit power and the information rate of \mathcal{B}_i , respectively. The fading gains between any pair of nodes in \mathcal{B}_i and $\mathcal{B}_{j'}$ are supposed to be independently drawn according to some distribution $f_{G_{\mathcal{B}_i, \mathcal{B}_{j'}}}(x)$.

The N cooperative infrastructure networks percolate if (10) holds. When without cooperation among the infrastructure networks, all the off-diagonal entries are zero. (10) decomposes and reduces to (4).

E. Cooperation among multiple wireless ad hoc networks and multiple infrastructure networks

In this subsection, we successively derive the degree distribution and the percolation condition of the heterogeneous network with cooperation among multiple ad hoc networks and multiple infrastructure networks. When infrastructure networks are available to carry and forward traffic for ad hoc networks, the network connectivity can be improved. For example, we may deploy sparsely wire connected relay stations to provide shortcuts for wireless traffic. As shown in Fig. 1, packets originated from nodes in ad hoc networks may be captured by nodes in infrastructure networks, and then forwarded via backhaul and broadcasted to other nodes in the ad hoc networks. With cooperation among M ad hoc networks and N infrastructure networks, the degree distribution of a node in \mathcal{A}_i becomes

$$\begin{aligned} p_{\mathcal{A}_i}(k_1, \dots, k_M, l_1, \dots, l_N) \\ = \frac{\exp(-\beta_{\mathcal{A}_i, \mathcal{A}_1}) \beta_{\mathcal{A}_i, \mathcal{A}_1}^{k_1}}{k_1!} \cdots \frac{\exp(-\beta_{\mathcal{A}_i, \mathcal{A}_M}) \beta_{\mathcal{A}_i, \mathcal{A}_M}^{k_M}}{k_M!} \\ \times \frac{\exp(-\beta_{\mathcal{A}_i, \mathcal{B}_1}) \beta_{\mathcal{A}_i, \mathcal{B}_1}^{l_1}}{l_1!} \cdots \frac{\exp(-\beta_{\mathcal{A}_i, \mathcal{B}_N}) \beta_{\mathcal{A}_i, \mathcal{B}_N}^{l_N}}{l_N!} \\ = \exp \left(- \sum_{j=1}^M \beta_{\mathcal{A}_i, \mathcal{A}_j} - \sum_{j'=1}^N \beta_{\mathcal{A}_i, \mathcal{B}_{j'}} \right) \\ \times \prod_{j=1}^M \frac{\beta_{\mathcal{A}_i, \mathcal{A}_j}^{k_j}}{k_j!} \prod_{j'=1}^N \frac{\beta_{\mathcal{A}_i, \mathcal{B}_{j'}}^{l_{j'}}}{l_{j'}!}, \\ k_j, l_{j'} = 0, 1, 2, \dots, 1 \leq j \leq M, 1 \leq j' \leq N \end{aligned} \quad (12)$$

where $\beta_{\mathcal{A}_i, \mathcal{A}_j}$ is defined in (6), and $\beta_{\mathcal{A}_i, \mathcal{B}_{j'}}$ is the average number of nodes in $\mathcal{B}_{j'}$ that can successfully decode the messages from the typical node of \mathcal{A}_i . $\beta_{\mathcal{A}_i, \mathcal{B}_{j'}}$ is computed as

$$\beta_{\mathcal{A}_i, \mathcal{B}_{j'}} = \frac{\lambda_{\mathcal{B}_{j'}} \pi P_{\mathcal{A}_i}^\delta \mathbb{E}[G_{\mathcal{A}_i, \mathcal{B}_{j'}}^\delta]}{(2^{R_{\mathcal{A}_i}} - 1)^\delta N_0^\delta}, \quad (13)$$

where the fading gains between any pair of nodes in \mathcal{A}_i and $\mathcal{B}_{j'}$ are supposed to be independently drawn according to some distribution $f_{G_{\mathcal{A}_i, \mathcal{B}_{j'}}}(x)$.

Similarly, packets originated from nodes in infrastructure networks may be forwarded via their wired backhaul connections as well as broadcasted by radio. In the latter case, the packets may be captured by nodes in ad hoc networks and other infrastructure networks. With cooperation among M ad hoc networks and N infrastructure networks, the degree

$$\begin{vmatrix} 1 - \frac{\sum_{l_1} [l_1^2 - l_1] p_{\mathcal{B}_1}(l_1)}{\sum_{l_1} l_1 p_{\mathcal{B}_1}(l_1)} & -\beta_{\mathcal{B}_1, \mathcal{B}_2} & \cdots & -\beta_{\mathcal{B}_1, \mathcal{B}_N} \\ -\beta_{\mathcal{B}_2, \mathcal{B}_1} & 1 - \frac{\sum_{l_2} [l_2^2 - l_2] p_{\mathcal{B}_2}(l_2)}{\sum_{l_2} l_2 p_{\mathcal{B}_2}(l_2)} & \cdots & -\beta_{\mathcal{B}_2, \mathcal{B}_N} \\ \vdots & \vdots & \ddots & \vdots \\ -\beta_{\mathcal{B}_N, \mathcal{B}_1} & -\beta_{\mathcal{B}_N, \mathcal{B}_2} & \cdots & 1 - \frac{\sum_{l_N} [l_N^2 - l_N] p_{\mathcal{B}_N}(l_N)}{\sum_{l_N} l_N p_{\mathcal{B}_N}(l_N)} \end{vmatrix} = 0. \quad (10)$$

$$\begin{vmatrix} 1 - \beta_{\mathcal{A}_1, \mathcal{A}_1} & \cdots & -\beta_{\mathcal{A}_1, \mathcal{A}_M} & -\beta_{\mathcal{A}_1, \mathcal{B}_1} & \cdots & -\beta_{\mathcal{A}_1, \mathcal{B}_N} \\ \vdots & \ddots & \vdots & \vdots & \ddots & \vdots \\ -\beta_{\mathcal{A}_M, \mathcal{A}_1} & \cdots & 1 - \beta_{\mathcal{A}_M, \mathcal{A}_M} & -\beta_{\mathcal{A}_M, \mathcal{B}_1} & \cdots & -\beta_{\mathcal{A}_M, \mathcal{B}_N} \\ -\beta_{\mathcal{B}_1, \mathcal{A}_1} & \cdots & -\beta_{\mathcal{B}_1, \mathcal{A}_M} & 1 - \frac{\sum_{l_1} [l_1^2 - l_1] p_{\mathcal{B}_1}(l_1)}{\sum_{l_1} l_1 p_{\mathcal{B}_1}(l_1)} & \cdots & -\beta_{\mathcal{B}_1, \mathcal{B}_N} \\ \vdots & \ddots & \vdots & \vdots & \ddots & \vdots \\ -\beta_{\mathcal{B}_N, \mathcal{A}_1} & \cdots & -\beta_{\mathcal{B}_N, \mathcal{A}_M} & -\beta_{\mathcal{B}_N, \mathcal{B}_1} & \cdots & 1 - \frac{\sum_{l_N} [l_N^2 - l_N] p_{\mathcal{B}_N}(l_N)}{\sum_{l_N} l_N p_{\mathcal{B}_N}(l_N)} \end{vmatrix} = 0. \quad (11)$$

distribution of a node in \mathcal{B}_i becomes

$$\begin{aligned} & p_{\mathcal{B}_i}(k_1, \dots, k_M, l_1, \dots, l_N) \\ &= p_{\mathcal{B}_i}(l_i) \exp \left(- \sum_{j=1}^M \beta_{\mathcal{B}_i, \mathcal{A}_j} - \sum_{j'=1, j' \neq i}^N \beta_{\mathcal{B}_i, \mathcal{B}_{j'}} \right) \\ & \times \prod_{j=1}^M \frac{\beta_{\mathcal{B}_i, \mathcal{A}_j}^{k_j}}{k_j!} \prod_{j'=1, j' \neq i}^N \frac{\beta_{\mathcal{B}_i, \mathcal{B}_{j'}}^{l_{j'}}}{l_{j'}!}, \\ & k_j, l_{j'} = 0, 1, 2, \dots, 1 \leq j \leq M, 1 \leq j' \leq N, \end{aligned} \quad (14)$$

where $\beta_{\mathcal{B}_i, \mathcal{B}_{j'}}$ is defined in (9), and $\beta_{\mathcal{B}_i, \mathcal{A}_j}$ is the average number of nodes in \mathcal{A}_j that can successfully decode the messages from the typical node of \mathcal{B}_i . $\beta_{\mathcal{B}_i, \mathcal{A}_j}$ is obtained as

$$\beta_{\mathcal{B}_i, \mathcal{A}_j} = \frac{\lambda_{\mathcal{A}_j} \pi P_{\mathcal{B}_i}^\delta \mathbb{E}[G_{\mathcal{B}_i, \mathcal{A}_j}^\delta]}{(2^{R_{\mathcal{B}_i}} - 1)^\delta N_0^\delta}, \quad (15)$$

where the fading gains between any pair of nodes in \mathcal{B}_i and \mathcal{A}_j are supposed to be independently drawn according to some distribution $f_{G_{\mathcal{B}_i, \mathcal{A}_j}}(x)$.

With cooperation among M ad hoc networks and N infrastructure networks, percolation happens when (11) holds. If there is no cooperation between the ad hoc networks and the infrastructure networks, the entries in the $M \times N$ block at the upper-right corner and the entries in the $N \times M$ block at the lower-left corner are all equal to zero. (11) decomposes and reduces to (7) and (10).

III. INTERFERENCE-LIMITED ENVIRONMENT

In this section, we derive the mean degree in consideration of both intra-system and inter-system interference. In addition, we assume that the M ad hoc networks and N infrastructure networks coexist with S interfering networks (representing primary networks and denoted as \mathcal{C}_s , $1 \leq s \leq S$). In other words, an ad hoc/infrastructure network node sustains interference from both concurrent transmissions in the ad hoc/infrastructure networks (using slotted ALOHA as medium

access strategies) and the S interfering networks. The main notations are summarized in Table I.

The medium access control for radio broadcasting in \mathcal{A}_i (\mathcal{B}_i) is supposed to be slotted ALOHA with medium access probability $p_{\mathcal{A}_i}$ ($p_{\mathcal{B}_i}$). By independent thinning $\Phi_{\mathcal{A}_i}$ ($\Phi_{\mathcal{B}_i}$) with probability $p_{\mathcal{A}_i}$ ($p_{\mathcal{B}_i}$), the set $\Phi_{\mathcal{A}_i}$ ($\Phi_{\mathcal{B}_i}$) is partitioned into two disjoint subsets $\Phi_{\mathcal{A}_i}^1$ ($\Phi_{\mathcal{B}_i}^1$) and $\Phi_{\mathcal{A}_i}^0$ ($\Phi_{\mathcal{B}_i}^0$). $\Phi_{\mathcal{A}_i}^1$ ($\Phi_{\mathcal{B}_i}^1$) denotes the transmitter PPP with density $p_{\mathcal{A}_i} \lambda_{\mathcal{A}_i}$ ($p_{\mathcal{B}_i} \lambda_{\mathcal{B}_i}$), and $\Phi_{\mathcal{A}_i}^0$ ($\Phi_{\mathcal{B}_i}^0$) denotes the receiver PPP with density $(1 - p_{\mathcal{A}_i}) \lambda_{\mathcal{A}_i}$ ($(1 - p_{\mathcal{B}_i}) \lambda_{\mathcal{B}_i}$). In addition, the interference from the active nodes in \mathcal{A}_m , $1 \leq m \leq M$, to the typical node of \mathcal{A}_i (\mathcal{B}_i) is denoted as $I_{\mathcal{A}_m, \mathcal{A}_i} = \sum_{x \in \Phi_{\mathcal{A}_m}^1} G_{\mathcal{A}_m, \mathcal{A}_i} P_{\mathcal{A}_m} \|x\|^{-\alpha}$ ($I_{\mathcal{A}_m, \mathcal{B}_i} = \sum_{x \in \Phi_{\mathcal{A}_m}^1} G_{\mathcal{A}_m, \mathcal{B}_i} P_{\mathcal{A}_m} \|x\|^{-\alpha}$). Similarly, the interference from the active nodes in \mathcal{B}_n , $1 \leq n \leq N$, to the typical node of \mathcal{A}_i (\mathcal{B}_i) is denoted as $I_{\mathcal{B}_n, \mathcal{A}_i} = \sum_{x \in \Phi_{\mathcal{B}_n}^1} G_{\mathcal{B}_n, \mathcal{A}_i} P_{\mathcal{B}_n} \|x\|^{-\alpha}$ ($I_{\mathcal{B}_n, \mathcal{B}_i} = \sum_{x \in \Phi_{\mathcal{B}_n}^1} G_{\mathcal{B}_n, \mathcal{B}_i} P_{\mathcal{B}_n} \|x\|^{-\alpha}$).

For the interfering networks, the spatial distribution of active nodes in \mathcal{C}_s is assumed to follow a PPP with density $\lambda_{\mathcal{C}_s}$. The set of locations of the active nodes in \mathcal{C}_s is denoted as $\Phi_{\mathcal{C}_s} = \{X_k^{\mathcal{C}_s}\}$ and the transmit power of a node is $P_{\mathcal{C}_s}$. The interference from the active nodes in \mathcal{C}_s to the typical node of \mathcal{A}_i (\mathcal{B}_i) is denoted as $I_{\mathcal{C}_s, \mathcal{A}_i} = \sum_{x \in \Phi_{\mathcal{C}_s}} G_{\mathcal{C}_s, \mathcal{A}_i} P_{\mathcal{C}_s} \|x\|^{-\alpha}$ ($I_{\mathcal{C}_s, \mathcal{B}_i} = \sum_{x \in \Phi_{\mathcal{C}_s}} G_{\mathcal{C}_s, \mathcal{B}_i} P_{\mathcal{C}_s} \|x\|^{-\alpha}$), where the fading gains between any pair of nodes in \mathcal{C}_s and \mathcal{A}_i (\mathcal{B}_i) are independently drawn according to some distribution $f_{G_{\mathcal{C}_s, \mathcal{A}_i}}(x)$ ($f_{G_{\mathcal{C}_s, \mathcal{B}_i}}(x)$).

A. Wireless ad hoc networks

In this subsection, we first derive the mean degree of an ad hoc network. Then, the percolation threshold is obtained following Section II.

In an interference-limited environment, neighbors of the typical node of \mathcal{A}_i are resulted from independent⁴ thinning of $x \in \Phi_{\mathcal{A}_i}^0$ with probability

⁴We assume that the spatial correlation of interference observed at different nodes in $\Phi_{\mathcal{A}_i}$ can be ignored due to the i.i.d. fading gains in different pairs of nodes [31]. However, the calculations of the mean degree in Theorem 1 still hold without this assumption.

$\mathbb{P}\left(\log\left(1 + \frac{G_{\mathcal{A}_i, \mathcal{A}_j} P_{\mathcal{A}_i} \|x\|^{-\alpha}}{\sum_{m=1}^M I_{\mathcal{A}_m, \mathcal{A}_i} + \sum_{n=1}^N I_{\mathcal{B}_n, \mathcal{A}_i} + \sum_{s=1}^S I_{\mathcal{C}_s, \mathcal{A}_i}}\right)\right) \geq R_{\mathcal{A}_i}$). By the mapping theorem, the number of one-hop neighbors of the typical node of \mathcal{A}_i is Poisson distributed with mean $\tilde{\beta}_{\mathcal{A}_i, \mathcal{A}_i}$. We have the following theorem.

Theorem 1. *Under general fading channels, $\tilde{\beta}_{\mathcal{A}_i, \mathcal{A}_i}$ can be computed in nearly closed-form as (16). $g_{\mathcal{A}_i, \mathcal{A}_i}(t)$ is the inverse Laplace transform of $\overline{F}_{G_{\mathcal{A}_i, \mathcal{A}_i}}(z)$ satisfying $\overline{F}_{G_{\mathcal{A}_i, \mathcal{A}_i}}(z) = \mathcal{L}\{g_{\mathcal{A}_i, \mathcal{A}_i}(t)\} = \int_{-\infty}^{\infty} e^{-zt} g_{\mathcal{A}_i, \mathcal{A}_i}(t) dt$, where $\overline{F}_{G_{\mathcal{A}_i, \mathcal{A}_i}}(z) = \mathbb{P}(G_{\mathcal{A}_i, \mathcal{A}_i} \geq z)$ is the ccdf (complementary cumulative distribution function) of the fading gain $G_{\mathcal{A}_i, \mathcal{A}_i}$. $\Gamma(z) = \int_0^{\infty} t^{z-1} e^{-t} dt$ is the Gamma function.*

Proof: The proof is presented in Appendix C. Closed-formed upper and lower bounds on $\tilde{\beta}_{\mathcal{A}_i, \mathcal{A}_i}$ can be carried out in a similar way as in [32]. Please note that there exists a trade-off between the mean degree $\tilde{\beta}_{\mathcal{A}_i, \mathcal{A}_i}$ (connectivity) and the medium access probability $p_{\mathcal{A}_i}$ (capacity). When the medium access probability increases, the intra-system interference increases, causing a reduction in the mean degree. ■

For example, when the desired signal is Nakagami- m faded with unit average power ($m = 1$ corresponds to Rayleigh fading), the ccdf of the fading gain $G_{\mathcal{A}_i, \mathcal{A}_i}$ is expressed as

$$\overline{F}_{G_{\mathcal{A}_i, \mathcal{A}_i}}(z) = e^{-mz} \sum_{k=0}^{m-1} \frac{(mz)^k}{k!}. \quad (18)$$

Its inverse Laplace transform can be computed as

$$g_{\mathcal{A}_i, \mathcal{A}_i}(t) = \sum_{k=0}^{m-1} \frac{m^k}{k!} \Delta^{(k)}(t-m), \quad (19)$$

where $\Delta^{(k)}(t)$ is the k -th derivative of Dirac delta function. We can therefore compute the expression

$$\begin{aligned} \int_{-\infty}^{\infty} g_{\mathcal{A}_i, \mathcal{A}_i}(t) t^{-\delta} dt &= \sum_{k=0}^{m-1} \frac{m^k}{k!} \int_{-\infty}^{\infty} \Delta^{(k)}(t-m) t^{-\delta} dt \\ &\stackrel{(a)}{=} m^{-\delta} \sum_{k=0}^{m-1} \frac{\prod_{i=0}^{k-1} (\delta+i)}{k!} \\ &= m^{-\delta} \sum_{k=0}^{m-1} \frac{\Gamma(\delta+k)}{\Gamma(\delta)\Gamma(k+1)}, \end{aligned} \quad (20)$$

where (a) follows the identity $\int_{-\infty}^{\infty} \Delta^{(k)}(x-c)\varphi(x)dx = (-1)^k \varphi^{(k)}(c)$, which can be obtained by integration by parts. $\varphi(x)$ is a test function.

In conclusion, the mean degree of ad hoc network \mathcal{A}_i in an interference-limited environment is $\tilde{\beta}_{\mathcal{A}_i, \mathcal{A}_i}$. The degree distribution and percolation threshold can be respectively derived by replacing $\beta_{\mathcal{A}_i, \mathcal{A}_i}$ in (2) and (3) with $\tilde{\beta}_{\mathcal{A}_i, \mathcal{A}_i}$.

B. Infrastructure networks

The degree distribution and percolation threshold of infrastructure network \mathcal{B}_i with wired backhaul connections remain the same as that of Section II-B.

C. Cooperation among multiple wireless ad hoc networks

With cooperation among M ad hoc networks, the degree distribution and percolation condition can be respectively

obtained by replacing $\beta_{\mathcal{A}_i, \mathcal{A}_j}$ in (5) and (7) with $\tilde{\beta}_{\mathcal{A}_i, \mathcal{A}_j}$. $\tilde{\beta}_{\mathcal{A}_i, \mathcal{A}_j}$ is computed as (17), where $g_{\mathcal{A}_i, \mathcal{A}_j}(t)$ is the inverse Laplace transform of $\overline{F}_{G_{\mathcal{A}_i, \mathcal{A}_j}}(z)$.

D. Cooperation among multiple infrastructure networks

With cooperation among N infrastructure networks, the degree distribution and percolation condition can be respectively obtained by replacing $\beta_{\mathcal{B}_i, \mathcal{B}_j}$ in (8) and (10) with $\tilde{\beta}_{\mathcal{B}_i, \mathcal{B}_j}$, which can be expressed in a similar form as (17).

E. Cooperation among multiple wireless ad hoc networks and multiple infrastructure networks

With cooperation among M ad hoc networks and N infrastructure networks, the degree distribution and percolation condition can be respectively obtained by replacing $\beta_{\mathcal{A}_i, \mathcal{A}_j}$, $\beta_{\mathcal{A}_i, \mathcal{B}_j}$, $\beta_{\mathcal{B}_i, \mathcal{B}_j}$, and $\beta_{\mathcal{B}_i, \mathcal{A}_j}$ in (12), (14), and (11) with $\tilde{\beta}_{\mathcal{A}_i, \mathcal{A}_j}$, $\tilde{\beta}_{\mathcal{A}_i, \mathcal{B}_j}$, $\tilde{\beta}_{\mathcal{B}_i, \mathcal{B}_j}$, and $\tilde{\beta}_{\mathcal{B}_i, \mathcal{A}_j}$, which can be expressed in a similar form as (17).

IV. COEXISTENCE OF PRIMARY NETWORKS AND SECONDARY NETWORKS

In this section, we study the performance degradation of secondary networks in terms of mean degrees and access probabilities when they coexist with primary networks. Suppose that the S interfering networks (denoted as \mathcal{C}_s , $1 \leq s \leq S$) in Section III are primary networks, and the M ad hoc networks (denoted as \mathcal{A}_m , $1 \leq m \leq M$) and N infrastructure networks (denoted as \mathcal{B}_n , $1 \leq n \leq N$) are secondary networks. In primary network \mathcal{C}_s , we assume that each active node (transmitter) $x \in \Phi_{\mathcal{C}_s}$ has a dedicated receiver at a fixed distance d_s^5 away with an arbitrary direction. As a result, the receiver nodes in primary network \mathcal{C}_s also form a PPP with density $\lambda_{\mathcal{C}_s}$. In addition, the fading gains between the transmitters and receivers (denoted as $G_{\mathcal{C}_s, \mathcal{C}_s}$) are supposed to be independently drawn from an exponential distribution (Rayleigh fading) with unit mean, without loss of generality. Furthermore, each receiver node in \mathcal{C}_s is assumed to have an outage constraint with maximum outage probability ϵ_s , and the information rate of a primary transmission is denoted as $R_{\mathcal{C}_s}$. The main notations are summarized in Table I.

The impacts of primary networks on the performance of secondary networks are two-fold. First, the quality of received signals at secondary networks is degraded due to the interference from transmitter nodes in primary network \mathcal{C}_s , $1 \leq s \leq S$, causing a reduction in the mean degree (and thus connectivity) of secondary networks, as addressed in Section III. Second, the interference from secondary networks to primary networks should be limited such that the outage constraints at receiver nodes in primary network \mathcal{C}_s , $1 \leq s \leq S$, are not violated. Specifically, the access probabilities $p_{\mathcal{A}_m}$, $1 \leq m \leq M$, and $p_{\mathcal{B}_n}$, $1 \leq n \leq N$, should satisfy the following outage constraints at primary networks as shown in (21), where (a) follows that $G_{\mathcal{C}_s, \mathcal{C}_s}$ is exponentially distributed with unit mean. After some simplifications, we observe that the constraints on the access probabilities $p_{\mathcal{A}_m}$, $1 \leq m \leq M$,

⁵The analysis can be easily generalized to the case that the distances between the transmitters and receivers are i.i.d.

$$\tilde{\beta}_{\mathcal{A}_i, \mathcal{A}_i} = \frac{(1 - p_{\mathcal{A}_i}) \lambda_{\mathcal{A}_i} P_{\mathcal{A}_i}^\delta \int_{-\infty}^{\infty} g_{\mathcal{A}_i, \mathcal{A}_i}(t) t^{-\delta} dt}{\left(\sum_{m=1}^M p_{\mathcal{A}_m} \lambda_{\mathcal{A}_m} P_{\mathcal{A}_m}^\delta \mathbb{E}[G_{\mathcal{A}_m, \mathcal{A}_i}^\delta] + \sum_{n=1}^N p_{\mathcal{B}_n} \lambda_{\mathcal{B}_n} P_{\mathcal{B}_n}^\delta \mathbb{E}[G_{\mathcal{B}_n, \mathcal{A}_i}^\delta] + \sum_{s=1}^S \lambda_{\mathcal{C}_s} P_{\mathcal{C}_s}^\delta \mathbb{E}[G_{\mathcal{C}_s, \mathcal{A}_i}^\delta] \right) (2^{R_{\mathcal{A}_i}} - 1)^\delta \Gamma(1 - \delta)} \quad (16)$$

$$\tilde{\beta}_{\mathcal{A}_i, \mathcal{A}_j} = \int_0^\infty (1 - p_{\mathcal{A}_j}) \lambda_{\mathcal{A}_j} \mathbb{P} \left(\log \left(1 + \frac{G_{\mathcal{A}_i, \mathcal{A}_j} P_{\mathcal{A}_i} r^{-\alpha}}{\sum_{m=1}^M I_{\mathcal{A}_m, \mathcal{A}_j} + \sum_{n=1}^N I_{\mathcal{B}_n, \mathcal{A}_j} + \sum_{s=1}^S I_{\mathcal{C}_s, \mathcal{A}_j}} \right) \geq R_{\mathcal{A}_i} \right) 2\pi r dr \quad (17)$$

$$= \frac{(1 - p_{\mathcal{A}_j}) \lambda_{\mathcal{A}_j} P_{\mathcal{A}_i}^\delta \int_{-\infty}^{\infty} g_{\mathcal{A}_i, \mathcal{A}_j}(t) t^{-\delta} dt}{\left(\sum_{m=1}^M p_{\mathcal{A}_m} \lambda_{\mathcal{A}_m} P_{\mathcal{A}_m}^\delta \mathbb{E}[G_{\mathcal{A}_m, \mathcal{A}_j}^\delta] + \sum_{n=1}^N p_{\mathcal{B}_n} \lambda_{\mathcal{B}_n} P_{\mathcal{B}_n}^\delta \mathbb{E}[G_{\mathcal{B}_n, \mathcal{A}_j}^\delta] + \sum_{s=1}^S \lambda_{\mathcal{C}_s} P_{\mathcal{C}_s}^\delta \mathbb{E}[G_{\mathcal{C}_s, \mathcal{A}_j}^\delta] \right) (2^{R_{\mathcal{A}_i}} - 1)^\delta \Gamma(1 - \delta)}$$

$$\mathbb{P} \left(\log \left(1 + \frac{G_{\mathcal{C}_s, \mathcal{C}_s} P_{\mathcal{C}_s} d_s^{-\alpha}}{\sum_{m=1}^M I_{\mathcal{A}_m, \mathcal{C}_s} + \sum_{n=1}^N I_{\mathcal{B}_n, \mathcal{C}_s} + \sum_{i=1}^S I_{\mathcal{C}_i, \mathcal{C}_s}} \right) < R_{\mathcal{C}_s} \right) \stackrel{(a)}{=} 1 - \exp \left\{ - \left(\sum_{m=1}^M p_{\mathcal{A}_m} \lambda_{\mathcal{A}_m} P_{\mathcal{A}_m}^\delta \mathbb{E}[G_{\mathcal{A}_m, \mathcal{C}_s}^\delta] + \sum_{n=1}^N p_{\mathcal{B}_n} \lambda_{\mathcal{B}_n} P_{\mathcal{B}_n}^\delta \mathbb{E}[G_{\mathcal{B}_n, \mathcal{C}_s}^\delta] + \sum_{i=1}^S \lambda_{\mathcal{C}_i} P_{\mathcal{C}_i}^\delta \mathbb{E}[G_{\mathcal{C}_i, \mathcal{C}_s}^\delta] \right) \pi d_s^2 (2^{R_{\mathcal{C}_s}} - 1)^\delta P_{\mathcal{C}_s}^{-\delta} \Gamma(1 - \delta) \right\} \leq \epsilon_s, \quad 1 \leq s \leq S. \quad (21)$$

and $p_{\mathcal{B}_n}$, $1 \leq n \leq N$, of secondary networks are linear. That is,

$$\sum_{m=1}^M p_{\mathcal{A}_m} \lambda_{\mathcal{A}_m} P_{\mathcal{A}_m}^\delta \mathbb{E}[G_{\mathcal{A}_m, \mathcal{C}_s}^\delta] + \sum_{n=1}^N p_{\mathcal{B}_n} \lambda_{\mathcal{B}_n} P_{\mathcal{B}_n}^\delta \mathbb{E}[G_{\mathcal{B}_n, \mathcal{C}_s}^\delta] \leq \frac{-\ln(1 - \epsilon_s)}{\pi d_s^2 (2^{R_{\mathcal{C}_s}} - 1)^\delta P_{\mathcal{C}_s}^{-\delta} \Gamma(1 - \delta)} - \sum_{i=1}^S \lambda_{\mathcal{C}_i} P_{\mathcal{C}_i}^\delta \mathbb{E}[G_{\mathcal{C}_i, \mathcal{C}_s}^\delta], \quad \forall s = 1, \dots, S;$$

$$0 \leq p_{\mathcal{A}_m} \leq 1, \quad \forall m = 1, 2, \dots, M;$$

$$0 \leq p_{\mathcal{B}_n} \leq 1, \quad \forall n = 1, 2, \dots, N. \quad (22)$$

These linear inequality constraints define the feasible region as a convex polyhedron, limiting the access probabilities of secondary networks. Note that the right-hand sides of the first S constraints should be positive, indicating that the interference from primary networks themselves is not strong enough to cause violation of the outage constraints at their receivers.

V. NUMERICAL RESULTS

Fig. 2 plots the degree distribution of wireless ad hoc network \mathcal{A}_i , $p_{\mathcal{A}_i}(k)$, in a noise-limited environment. The fading channel models include Rayleigh fading, Nakagami- m ($m = 3$) fading, and without fading (only path loss effect). All of them are with unit average power. Under Rayleigh fading, Nakagami- m fading, and without fading, we respectively have $\beta_{\mathcal{A}_i, \mathcal{A}_i} = 7.2$, $\beta_{\mathcal{A}_i, \mathcal{A}_i} = 7.8$, and $\beta_{\mathcal{A}_i, \mathcal{A}_i} = 8.1$. It can be observed that when the multiple path effect is less severe, $\beta_{\mathcal{A}_i, \mathcal{A}_i}$ becomes larger. Fig. 3 further shows that the mean degree $\beta_{\mathcal{A}_i, \mathcal{A}_i}$ increases with the transmit power $P_{\mathcal{A}_i}$ under different fading channel models.

Fig. 4 illustrates percolation of wireless ad hoc network \mathcal{A}_i . The relationship between the mean degree $\beta_{\mathcal{A}_i, \mathcal{A}_i}$ and transmit power $P_{\mathcal{A}_i}$ is shown. When $\beta_{\mathcal{A}_i, \mathcal{A}_i} = 1$ (or equivalently, $P_{\mathcal{A}_i} = 0.019$), the ad hoc network \mathcal{A}_i percolates and the mean component size reachable from a randomly selected node in \mathcal{A}_i blows up, indicating the formation of an infinite connected

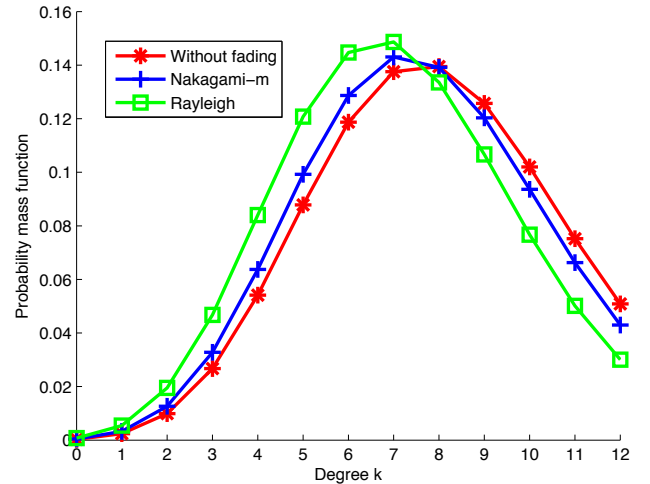


Fig. 2. $p_{\mathcal{A}_i}(k)$ is plotted under different fading channel models. The system parameters are set as $\lambda_{\mathcal{A}_i} = 10^{-3}$, $R_{\mathcal{A}_i} = 4$, $P_{\mathcal{A}_i} = 1$, $N_0 = 10^{-8}$, and $\alpha = 4$. Both Rayleigh and Nakagami- m ($m = 3$) fading are with unit average power.

component. Note that the mean component size $H'_0(1)$ is proportional to $1/(1 - \beta_{\mathcal{A}_i, \mathcal{A}_i})$ as indicated in Appendix A.

Fig. 5 and Fig. 6 demonstrate the benefit of cooperation between two wireless ad hoc networks \mathcal{A}_1 and \mathcal{A}_2 . Let $\det(\mathbf{Q}) \triangleq \begin{vmatrix} 1 - \beta_{\mathcal{A}_1, \mathcal{A}_1} & -\beta_{\mathcal{A}_1, \mathcal{A}_2} \\ -\beta_{\mathcal{A}_2, \mathcal{A}_1} & 1 - \beta_{\mathcal{A}_2, \mathcal{A}_2} \end{vmatrix}$. As shown in Fig. 5, when $P_{\mathcal{A}_1} (= P_{\mathcal{A}_2})$ increases, all $\beta_{\mathcal{A}_1, \mathcal{A}_1}$, $\beta_{\mathcal{A}_1, \mathcal{A}_2}$, $\beta_{\mathcal{A}_2, \mathcal{A}_1}$, and $\beta_{\mathcal{A}_2, \mathcal{A}_2}$ increase. With cooperation between \mathcal{A}_1 and \mathcal{A}_2 , the mean component size reachable from a randomly selected node in \mathcal{A}_1 or \mathcal{A}_2 , which is proportional to $1/\det(\mathbf{Q})$ as shown in Appendix B, blows up when the first zero of $\det(\mathbf{Q})$ is reached, indicating the formation of an infinite connected component. In other words, percolation of the cooperative network happens when $\det(\mathbf{Q}) = (1 - \beta_{\mathcal{A}_1, \mathcal{A}_1})(1 - \beta_{\mathcal{A}_2, \mathcal{A}_2}) - \beta_{\mathcal{A}_1, \mathcal{A}_2} \beta_{\mathcal{A}_2, \mathcal{A}_1} = 0$ at $P_{\mathcal{A}_1} = P_{\mathcal{A}_2} = 0.009$. As illustrated in Fig. 6, without cooperation, \mathcal{A}_1 percolates when $\beta_{\mathcal{A}_1, \mathcal{A}_1} = 1$

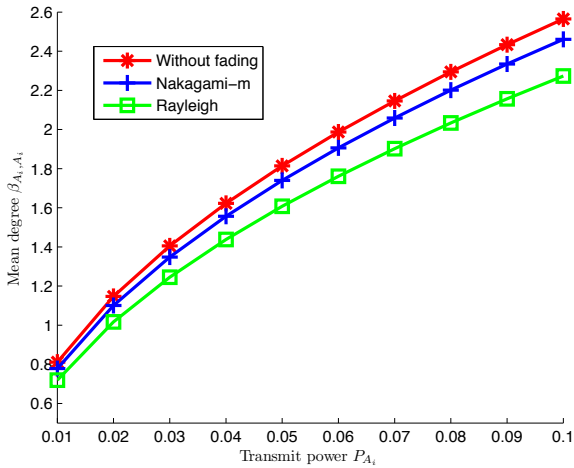


Fig. 3. The mean degree $\beta_{\mathcal{A}_i, \mathcal{A}_i}$ is plotted with respect to the transmit power $P_{\mathcal{A}_i}$ under different fading channel models. The system parameters are set as $\lambda_{\mathcal{A}_i} = 10^{-3}$, $R_{\mathcal{A}_i} = 4$, $N_0 = 10^{-8}$, and $\alpha = 4$. $P_{\mathcal{A}_i}$ is varied from 0.01 to 0.1. Both Rayleigh and Nakagami- m ($m = 3$) fading are with unit average power.

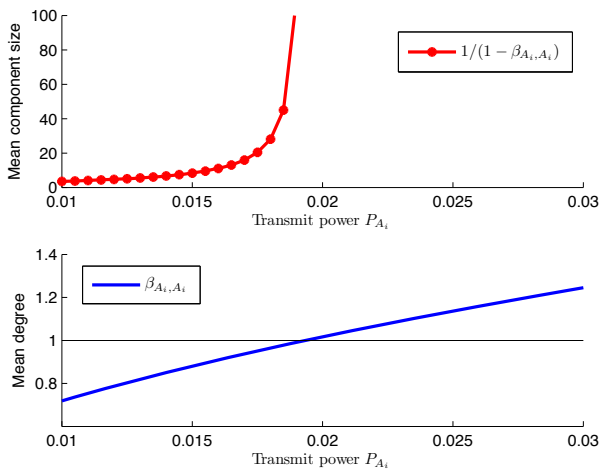


Fig. 4. Percolation of \mathcal{A}_i happens (or the mean component size blows up) when the mean degree $\beta_{\mathcal{A}_i, \mathcal{A}_i} = 1$. The system parameters are set as $\lambda_{\mathcal{A}_i} = 10^{-3}$, $R_{\mathcal{A}_i} = 4$, $N_0 = 10^{-8}$, and $\alpha = 4$. $P_{\mathcal{A}_i}$ is varied from 0.01 to 0.03. The channel is Rayleigh faded with unit average power.

at $P_{\mathcal{A}_1} = 0.019$, and \mathcal{A}_2 percolates when $\beta_{\mathcal{A}_2, \mathcal{A}_2} = 1$ at $P_{\mathcal{A}_2} = 0.037$. Note that $\beta_{\mathcal{A}_1, \mathcal{A}_2} = \beta_{\mathcal{A}_2, \mathcal{A}_1} = 0$ when there is no cooperation between \mathcal{A}_1 and \mathcal{A}_2 . This example could have two interpretations. First, when the stand-alone ad hoc network \mathcal{A}_1 or \mathcal{A}_2 operates with transmit power below percolation threshold, e.g., $P_{\mathcal{A}_1} = P_{\mathcal{A}_2} = 0.015$, percolation will occur only when both \mathcal{A}_1 and \mathcal{A}_2 cooperate with each other by using other network's nodes as relays. Second, when both \mathcal{A}_1 and \mathcal{A}_2 percolate with $P_{\mathcal{A}_1} = 0.019$ and $P_{\mathcal{A}_2} = 0.037$, percolation occurs much earlier (at $P_{\mathcal{A}_1} = P_{\mathcal{A}_2} = 0.009$) with cooperation between \mathcal{A}_1 and \mathcal{A}_2 , suggesting that both networks can operate at lower transmit power to sustain the same level of connectivity. Power efficiency is improved.

In Fig. 7 and Fig. 8, we further consider the case with cooperation among three ad hoc networks \mathcal{A}_1 , \mathcal{A}_2 , and \mathcal{A}_3 . Fig. 7 shows that percolation of the cooperative ad hoc

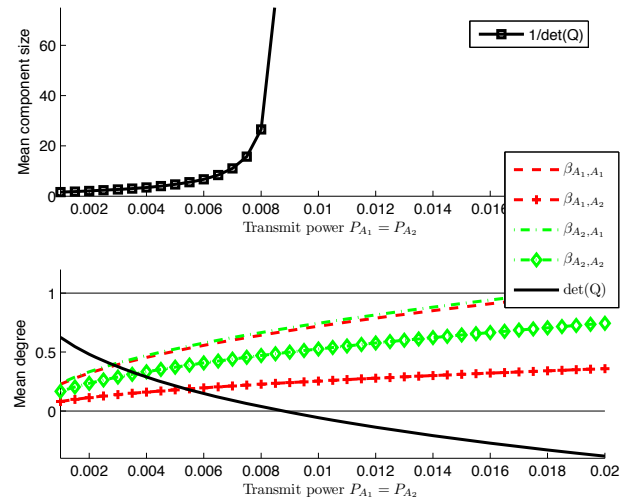


Fig. 5. With cooperation between ad hoc networks \mathcal{A}_1 and \mathcal{A}_2 , percolation happens when $\det(\mathbf{Q}) = (1 - \beta_{\mathcal{A}_1, \mathcal{A}_1})(1 - \beta_{\mathcal{A}_2, \mathcal{A}_2}) - \beta_{\mathcal{A}_1, \mathcal{A}_2}\beta_{\mathcal{A}_2, \mathcal{A}_1} = 0$. The system parameters are set as $\lambda_{\mathcal{A}_1} = 10^{-3}$, $R_{\mathcal{A}_1} = 4$, $\lambda_{\mathcal{A}_2} = 5 \times 10^{-4}$, $R_{\mathcal{A}_2} = 3$, $N_0 = 10^{-8}$, and $\alpha = 4$. Both $P_{\mathcal{A}_1}$ and $P_{\mathcal{A}_2}$ are varied simultaneously from 0.001 to 0.02. The channels in \mathcal{A}_1 or \mathcal{A}_2 are Rayleigh faded with unit average power, while the channels across \mathcal{A}_1 and \mathcal{A}_2 are Rayleigh faded with average power 0.5.

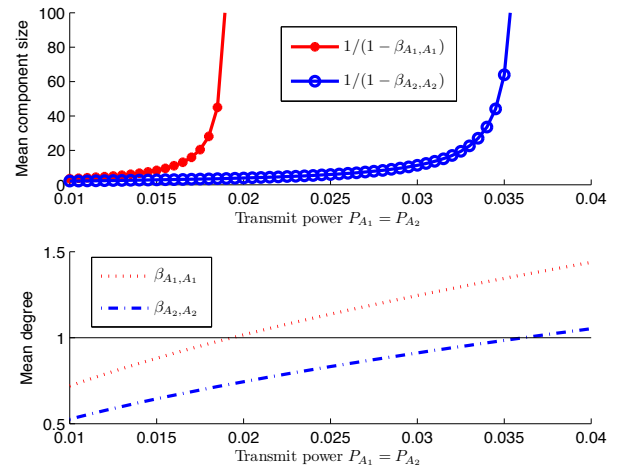


Fig. 6. Without cooperation, percolation of \mathcal{A}_1 (resp. \mathcal{A}_2) happens when the mean degree $\beta_{\mathcal{A}_1, \mathcal{A}_1} = 1$ (resp. $\beta_{\mathcal{A}_2, \mathcal{A}_2} = 1$). The system parameters are the same as in Fig. 5.

network happens when $P_{\mathcal{A}_1} = P_{\mathcal{A}_2} = P_{\mathcal{A}_3} = 0.02$ (corresponding to $\det(\mathbf{Q}) = 0$). However, without cooperation, much higher transmit power is required for percolation of \mathcal{A}_1 (at $P_{\mathcal{A}_1} = 0.08$), \mathcal{A}_2 (at $P_{\mathcal{A}_2} = 0.22$), and \mathcal{A}_3 (at $P_{\mathcal{A}_3} = 0.48$), as shown in Fig. 8.

Fig. 9 considers cooperation between a weakly-connected ad hoc network \mathcal{A}_1 and an infrastructure network \mathcal{B}_1 , and investigates the amount of infrastructure to be deployed to facilitate percolation of the ad hoc network. The infrastructure nodes are connected with wired backhaul, whose degree distribution is supposed to follow a geometric distribution with parameter p , i.e., $p_{\mathcal{B}_1}(k) = (1 - p)^k p$, $k = 0, 1, 2, \dots$. We would decide the parameter p that characterizes the

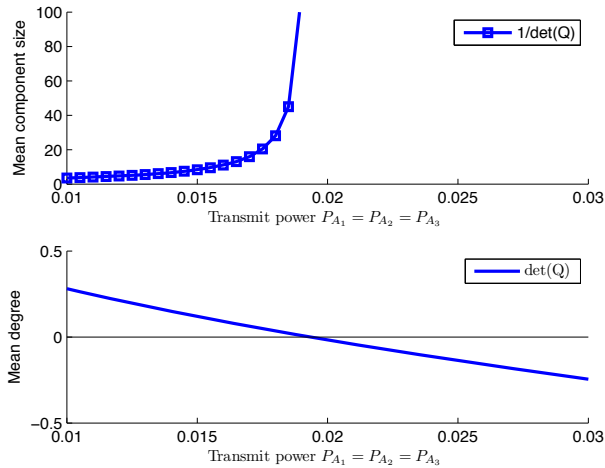


Fig. 7. With cooperation among ad hoc networks \mathcal{A}_1 , \mathcal{A}_2 , and \mathcal{A}_3 , percolation happens when $\det(\mathbf{Q}) = 0$ with $P_{\mathcal{A}_1} = P_{\mathcal{A}_2} = P_{\mathcal{A}_3} = 0.02$. The system parameters are set as $\lambda_{\mathcal{A}_1} = 5 \times 10^{-4}$, $\lambda_{\mathcal{A}_2} = 3 \times 10^{-4}$, $\lambda_{\mathcal{A}_3} = 2 \times 10^{-4}$, $R_{\mathcal{A}_1} = R_{\mathcal{A}_2} = R_{\mathcal{A}_3} = 4$, $N_0 = 10^{-8}$, and $\alpha = 4$. $P_{\mathcal{A}_1}$, $P_{\mathcal{A}_2}$, and $P_{\mathcal{A}_3}$ are varied simultaneously. All links are Rayleigh faded with unit average power.

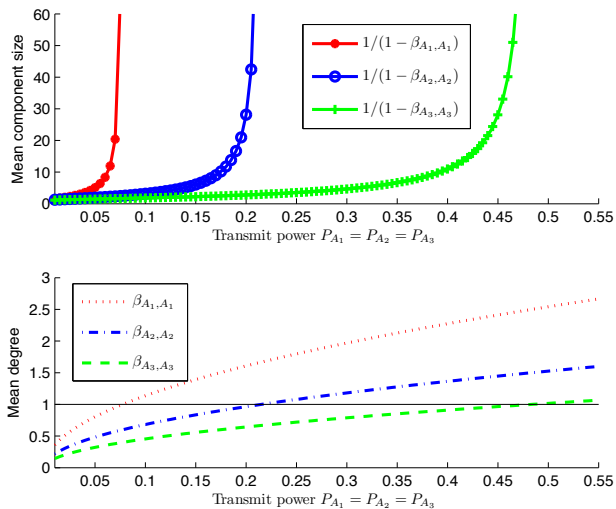


Fig. 8. Without cooperation, percolation of \mathcal{A}_1 , \mathcal{A}_2 , and \mathcal{A}_3 happens when the mean degree $\beta_{\mathcal{A}_1, \mathcal{A}_1} = 1$ at $P_{\mathcal{A}_1} = 0.08$, $\beta_{\mathcal{A}_2, \mathcal{A}_2} = 1$ at $P_{\mathcal{A}_2} = 0.22$, and $\beta_{\mathcal{A}_3, \mathcal{A}_3} = 1$ at $P_{\mathcal{A}_3} = 0.48$. The system parameters are the same as in Fig. 7.

amount of wired backhaul connections among infrastructure nodes. Note that when p decreases from 1 to 0, the amount of wired backhaul connections increases. By solving $\det(\mathbf{Q}) \triangleq \begin{vmatrix} 1 - \beta_{\mathcal{A}_1, \mathcal{A}_1} & -\beta_{\mathcal{A}_1, \mathcal{B}_1} \\ -\beta_{\mathcal{B}_1, \mathcal{A}_1} & 1 - \frac{\sum_{k=0}^{\infty} [k^2 - k] p_{\mathcal{B}_1}(k)}{\sum_{k=0}^{\infty} k p_{\mathcal{B}_1}(k)} \end{vmatrix} = (1 - \beta_{\mathcal{A}_1, \mathcal{A}_1})(1 - \frac{2-2p}{p}) - \beta_{\mathcal{A}_1, \mathcal{B}_1} \beta_{\mathcal{B}_1, \mathcal{A}_1} = 0$, we have $p = 2 \left(3 - \frac{\beta_{\mathcal{A}_1, \mathcal{B}_1} \beta_{\mathcal{B}_1, \mathcal{A}_1}}{1 - \beta_{\mathcal{A}_1, \mathcal{A}_1}} \right)^{-1}$. Given the system parameters as shown in Fig. 9, percolation of ad hoc network \mathcal{A}_1 happens when $p = 0.83$. Please note that $\beta_{\mathcal{A}_1, \mathcal{A}_1}$, $\beta_{\mathcal{A}_1, \mathcal{B}_1}$, and $\beta_{\mathcal{B}_1, \mathcal{A}_1}$ do not depend on the parameter p .

Fig. 10 plots the mean degree of wireless ad hoc network \mathcal{A}_i with respect to transmit power $P_{\mathcal{A}_i}$ in an interference-limited

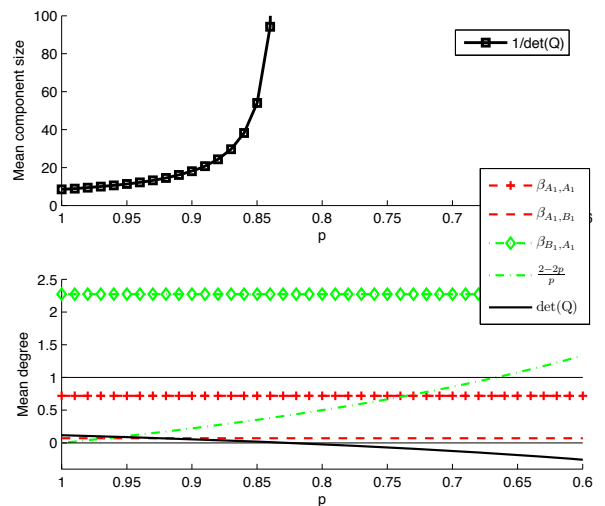


Fig. 9. With cooperation between an ad hoc network \mathcal{A}_1 and an infrastructure network \mathcal{B}_1 , percolation happens when $\det(\mathbf{Q}) = (1 - \beta_{\mathcal{A}_1, \mathcal{A}_1})(1 - \frac{2-2p}{p}) - \beta_{\mathcal{A}_1, \mathcal{B}_1} \beta_{\mathcal{B}_1, \mathcal{A}_1} = 0$. The system parameters are set as $\lambda_{\mathcal{A}_1} = 10^{-3}$, $R_{\mathcal{A}_1} = 4$, $P_{\mathcal{A}_1} = 0.01$, $\lambda_{\mathcal{B}_1} = 10^{-4}$, $R_{\mathcal{B}_1} = 4$, $P_{\mathcal{B}_1} = 0.1$, $N_0 = 10^{-8}$, and $\alpha = 4$. The parameter p is varied from 1 to 0.6. All links are Rayleigh faded with unit average power.

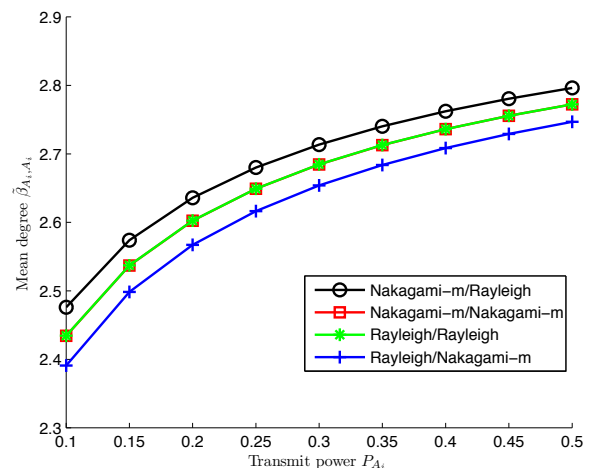


Fig. 10. The mean degree $\tilde{\beta}_{\mathcal{A}_i, \mathcal{A}_i}$ is plotted with respect to the transmit power $P_{\mathcal{A}_i}$ under different fading channel models. The notation “Nakagami- m /Rayleigh” represents that $G_{\mathcal{A}_i, \mathcal{A}_i}$ is subject to Nakagami- m ($m = 3$) fading and $G_{\mathcal{C}_1, \mathcal{A}_i}$ is subject to Rayleigh fading. Both Rayleigh and Nakagami- m fading are with unit average power. The system parameters are set as $p_{\mathcal{A}_i} = 0.05$, $\lambda_{\mathcal{A}_i} = 10^{-3}$, $R_{\mathcal{A}_i} = 4$, $\alpha = 4$, $S = 1$, $\lambda_{\mathcal{C}_1} = 10^{-5}$, and $P_{\mathcal{C}_1} = 0.2$. $P_{\mathcal{A}_i}$ is varied from 0.1 to 0.5.

environment under different fading channel models. It can be observed that $\tilde{\beta}_{\mathcal{A}_i, \mathcal{A}_i}$ in case “Nakagami- m /Rayleigh” $>$ $\tilde{\beta}_{\mathcal{A}_i, \mathcal{A}_i}$ in case “Nakagami- m /Nakagami- m ” \approx $\tilde{\beta}_{\mathcal{A}_i, \mathcal{A}_i}$ in case “Rayleigh/Rayleigh” $>$ $\tilde{\beta}_{\mathcal{A}_i, \mathcal{A}_i}$ in case “Rayleigh/Nakagami- m ”.

VI. CONCLUSION

As the most general CRN scenario, by sharing the same spectrum, multiple ad hoc networks and multiple infrastructure networks form a heterogeneous network, cooperating with

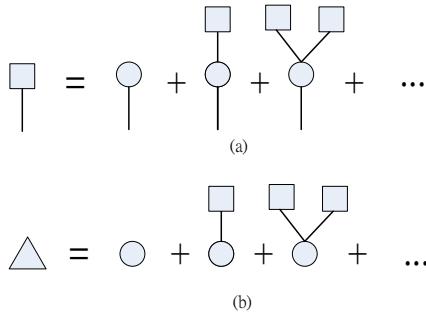


Fig. 11. (a) An illustration of the self-consistency relation $H_1(x) = x \sum_{k=0}^{\infty} q_{\mathcal{A}_i}(k)(H_1(x))^k = xF_1(H_1(x))$. A square represents the connected component reachable by following a randomly selected link, and a circle represents the node first reached. The component size can be expressed as the sum of the probabilities of having only a single node, having a single node connected to one other component, etc. (b) An illustration of the relation $H_0(x) = x \sum_{k=0}^{\infty} p_{\mathcal{A}_i}(k)(H_1(x))^k = xF_0(H_1(x))$. The triangle represents the connected component reachable by following a randomly selected node.

each other by using other networks' nodes as relays to carry and forward data traffic. In this paper, we analyzed the connectivity of the heterogeneous network from a percolation-based perspective, in both noise-limited and interference-limited environment with general fading channels.

The percolation threshold of a stand-alone ad hoc/infrastructure network was generalized to the determinant criterion in the cooperative case, quantifying the benefit of network-based cooperation. With such quantification, network deployment and control can be facilitated. As shown in the numerical results, when the two ad hoc networks do not percolate, percolation can occur with cooperation. In addition, when the two ad hoc networks percolate, we computed the transmit power that can be saved with cooperation, sustaining the same level of connectivity. Furthermore, we specified the amount of wired backhaul connections among infrastructure nodes to be deployed to facilitate percolation of an ad hoc network. Dedicated communication links in the infrastructure act as a mean to control the overall network connectivity. Finally, we applied the results to the coexistence of primary and secondary networks, where the outage constraints at primary receivers confine the access probabilities of secondary networks to a convex polyhedron.

Future work could investigate the increase in the fraction of the infinite connected component (rather than analyzing the percolation threshold) with network-based cooperation in the supercritical phase.

APPENDIX A PROOF OF PROPOSITION 1

We first define the generating function of the degree of a randomly selected node in \mathcal{A}_i as $F_0(x) = \sum_{k=0}^{\infty} p_{\mathcal{A}_i}(k)x^k$. Then, we define the excess degree⁶ distribution of a node at the end of a randomly selected link as $q_{\mathcal{A}_i}(k)$. Since it is more likely to arrive at a node that has a higher degree by following a randomly selected link, $q_{\mathcal{A}_i}(k) = [k+1]p_{\mathcal{A}_i}(k+1) / \sum_k kp_{\mathcal{A}_i}(k) = [k+1]p_{\mathcal{A}_i}(k+1) / \beta_{\mathcal{A}_i, \mathcal{A}_i}$, being proportional to $k p_{\mathcal{A}_i}(k)$ [33]. The generating function of $q_{\mathcal{A}_i}(k)$ is

⁶Excess degree of a node is one less than its total degree.

defined as $F_1(x) = \sum_{k=0}^{\infty} q_{\mathcal{A}_i}(k)x^k$, and we can easily verify that $F_1(x) = F_0'(x) / \beta_{\mathcal{A}_i, \mathcal{A}_i}$, where $F_0'(x)$ denotes the derivative of $F_0(x)$. Moreover, the generating function of a randomly selected link is defined as $H_1(x)$, which satisfies the self-consistency relation $H_1(x) = x \sum_{k=0}^{\infty} q_{\mathcal{A}_i}(k)(H_1(x))^k = xF_1(H_1(x))$. An illustration is provided in Fig. 11(a). In addition, the generating function of the total number of nodes reachable by following a randomly selected node is defined as $H_0(x)$, which satisfies the relation $H_0(x) = x \sum_{k=0}^{\infty} p_{\mathcal{A}_i}(k)(H_1(x))^k = xF_0(H_1(x))$. An illustration is provided in Fig. 11(b). More details can be found in [27], [33].

Consequently, the average total number of nodes (or the mean component size) reachable from a randomly selected node in \mathcal{A}_i is $H_0'(1) = 1 + \frac{F_0'(1)}{1-F_1'(1)}$, which blows up when $1 - F_1'(1) = 1 - \frac{\sum_{k=0}^{\infty} [k^2 - k] p_{\mathcal{A}_i}(k)}{\sum_{k=0}^{\infty} k p_{\mathcal{A}_i}(k)} = 0$, indicating the formation of an infinite connected component in \mathcal{A}_i . Here in the Poisson case with (2), we have $F_0(x) = F_1(x) = \exp(\beta_{\mathcal{A}_i, \mathcal{A}_i}(x-1))$. The percolation threshold is obtained by solving $1 - F_1'(1) = 1 - \beta_{\mathcal{A}_i, \mathcal{A}_i} = 0$, and we have $\beta_{\mathcal{A}_i, \mathcal{A}_i}^c = 1$.

APPENDIX B PROOF OF PROPOSITION 2

To obtain the percolation condition of the cooperative ad hoc networks, we follow the procedure described in Appendix A. First, the degree distribution of a randomly selected node in \mathcal{A}_i is denoted as $p_{\mathcal{A}_i}(k_1, k_2, \dots, k_M)$, $1 \leq i \leq M$, which has been computed in (5) as

$$p_{\mathcal{A}_i}(k_1, k_2, \dots, k_M) = \exp\left(-\sum_{j=1}^M \beta_{\mathcal{A}_i, \mathcal{A}_j}\right) \prod_{j=1}^M \frac{\beta_{\mathcal{A}_i, \mathcal{A}_j}^{k_j}}{k_j!},$$

$$k_j = 0, 1, 2, \dots, 1 \leq j \leq M. \quad (23)$$

The generating function of $p_{\mathcal{A}_i}(k_1, \dots, k_M)$ is defined as $F_0^{\mathcal{A}_i}(x_1, \dots, x_M)$, $1 \leq i \leq M$, which can be derived as

$$F_0^{\mathcal{A}_i}(x_1, \dots, x_M) = \sum_{k_1, \dots, k_M=0}^{\infty} p_{\mathcal{A}_i}(k_1, \dots, k_M) x_1^{k_1} \dots x_M^{k_M}$$

$$= \exp\left(\sum_{j=1}^M \beta_{\mathcal{A}_i, \mathcal{A}_j}(x_j - 1)\right). \quad (24)$$

Second, the excess degree distribution of a node in \mathcal{A}_i , which we reach by following a randomly selected link originated at a node of \mathcal{A}_j , is defined as $q_{\mathcal{A}_j \rightarrow \mathcal{A}_i}(k_1, \dots, k_M)$, $1 \leq j \leq M$, $1 \leq i \leq M$. We have

$$q_{\mathcal{A}_j \rightarrow \mathcal{A}_i}(k_1, \dots, k_M)$$

$$= (k_j + 1) p_{\mathcal{A}_i}(k_1, \dots, k_{j-1}, k_j + 1, k_{j+1}, \dots, k_M)$$

$$\Bigg/ \sum_{k_1, \dots, k_M=0}^{\infty} k_j p_{\mathcal{A}_i}(k_1, \dots, k_M)$$

$$\stackrel{(a)}{=} p_{\mathcal{A}_i}(k_1, \dots, k_M), \quad (27)$$

where (a) follows (23). From (27), it can be observed that in the Poisson case, the excess degree distribution is the same as the degree distribution, which does

$$\begin{aligned} \begin{bmatrix} H_0^{\mathcal{A}_1}(1) \\ \vdots \\ H_0^{\mathcal{A}_M}(1) \end{bmatrix} &\stackrel{(a)}{=} \begin{bmatrix} 1 \\ \vdots \\ 1 \end{bmatrix} + \begin{bmatrix} \beta_{\mathcal{A}_1, \mathcal{A}_1} & \cdots & \beta_{\mathcal{A}_1, \mathcal{A}_M} \\ \vdots & \ddots & \vdots \\ \beta_{\mathcal{A}_M, \mathcal{A}_1} & \cdots & \beta_{\mathcal{A}_M, \mathcal{A}_M} \end{bmatrix} \begin{bmatrix} H_1^{\mathcal{A}_1}(1) \\ \vdots \\ H_1^{\mathcal{A}_M}(1) \end{bmatrix} \\ &\stackrel{(b)}{=} \begin{bmatrix} 1 \\ \vdots \\ 1 \end{bmatrix} + \begin{bmatrix} \beta_{\mathcal{A}_1, \mathcal{A}_1} & \cdots & \beta_{\mathcal{A}_1, \mathcal{A}_M} \\ \vdots & \ddots & \vdots \\ \beta_{\mathcal{A}_M, \mathcal{A}_1} & \cdots & \beta_{\mathcal{A}_M, \mathcal{A}_M} \end{bmatrix} \begin{bmatrix} 1 - \beta_{\mathcal{A}_1, \mathcal{A}_1} & \cdots & -\beta_{\mathcal{A}_1, \mathcal{A}_M} \\ \vdots & \ddots & \vdots \\ -\beta_{\mathcal{A}_M, \mathcal{A}_1} & \cdots & 1 - \beta_{\mathcal{A}_M, \mathcal{A}_M} \end{bmatrix}^{-1} \begin{bmatrix} 1 \\ \vdots \\ 1 \end{bmatrix}. \end{aligned} \quad (25)$$

$$\begin{vmatrix} 1 - \frac{\sum_{k_1=0}^{\infty} [k_1^2 - k_1] p_{\mathcal{A}_1}(k_1)}{\sum_{k_1=0}^{\infty} k_1 p_{\mathcal{A}_1}(k_1)} & -\frac{\sum_{k_2=0}^{\infty} [k_2^2 - k_2] p_{\mathcal{A}_1}(k_2)}{\sum_{k_2=0}^{\infty} k_2 p_{\mathcal{A}_1}(k_2)} & \cdots & -\frac{\sum_{k_M=0}^{\infty} [k_M^2 - k_M] p_{\mathcal{A}_1}(k_M)}{\sum_{k_M=0}^{\infty} k_M p_{\mathcal{A}_1}(k_M)} \\ -\frac{\sum_{k_1=0}^{\infty} [k_1^2 - k_1] p_{\mathcal{A}_2}(k_1)}{\sum_{k_1=0}^{\infty} k_1 p_{\mathcal{A}_2}(k_1)} & 1 - \frac{\sum_{k_2=0}^{\infty} [k_2^2 - k_2] p_{\mathcal{A}_2}(k_2)}{\sum_{k_2=0}^{\infty} k_2 p_{\mathcal{A}_2}(k_2)} & \cdots & -\frac{\sum_{k_M=0}^{\infty} [k_M^2 - k_M] p_{\mathcal{A}_2}(k_M)}{\sum_{k_M=0}^{\infty} k_M p_{\mathcal{A}_2}(k_M)} \\ \vdots & \vdots & \ddots & \vdots \\ -\frac{\sum_{k_1=0}^{\infty} [k_1^2 - k_1] p_{\mathcal{A}_M}(k_1)}{\sum_{k_1=0}^{\infty} k_1 p_{\mathcal{A}_M}(k_1)} & -\frac{\sum_{k_2=0}^{\infty} [k_2^2 - k_2] p_{\mathcal{A}_M}(k_2)}{\sum_{k_2=0}^{\infty} k_2 p_{\mathcal{A}_M}(k_2)} & \cdots & 1 - \frac{\sum_{k_M=0}^{\infty} [k_M^2 - k_M] p_{\mathcal{A}_M}(k_M)}{\sum_{k_M=0}^{\infty} k_M p_{\mathcal{A}_M}(k_M)} \end{vmatrix} = 0. \quad (26)$$

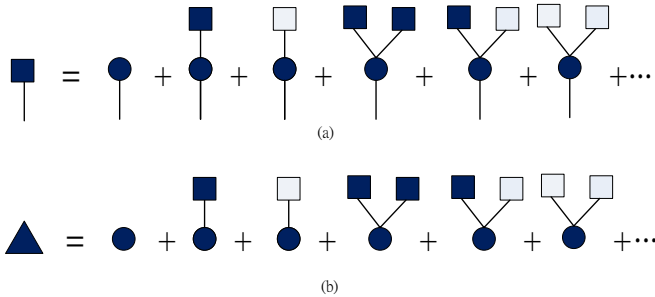


Fig. 12. An example with two networks \mathcal{A}_1 and \mathcal{A}_2 . (a) It illustrates the self-consistency relation $H_1^{\mathcal{A}_1}(x) = x \sum_{k_1, k_2=0}^{\infty} q_{\mathcal{A}_1}(k_1, k_2) [H_1^{\mathcal{A}_1}(x)]^{k_1} [H_1^{\mathcal{A}_2}(x)]^{k_2} = x F_1^{\mathcal{A}_1}(H_1^{\mathcal{A}_1}(x), H_1^{\mathcal{A}_2}(x))$. A dark (light) color square represents the connected component of nodes reached by following a randomly selected link that arrives at a node of \mathcal{A}_1 (\mathcal{A}_2). A dark (light) color circle represents the node of \mathcal{A}_1 that we first reach. (b) It illustrates the relation $H_0^{\mathcal{A}_1}(x) = x \sum_{k_1, k_2=0}^{\infty} p_{\mathcal{A}_1}(k_1, k_2) [H_1^{\mathcal{A}_1}(x)]^{k_1} [H_1^{\mathcal{A}_2}(x)]^{k_2} = x F_0^{\mathcal{A}_1}(H_1^{\mathcal{A}_1}(x), H_1^{\mathcal{A}_2}(x))$. The dark color triangle represents the connected component reachable by following a randomly selected node of \mathcal{A}_1 .

not depend on the index j . As a result, for simplification, we let $q_{\mathcal{A}_j \rightarrow \mathcal{A}_i}(k_1, \dots, k_M) \triangleq q_{\mathcal{A}_i}(k_1, \dots, k_M)$. The generating function of $q_{\mathcal{A}_i}(k_1, \dots, k_M)$ is defined as $F_1^{\mathcal{A}_i}(x_1, \dots, x_M)$, $1 \leq i \leq M$, which can be computed as

$$\begin{aligned} F_1^{\mathcal{A}_i}(x_1, \dots, x_M) &= \sum_{k_1, \dots, k_M=0}^{\infty} q_{\mathcal{A}_i}(k_1, \dots, k_M) x_1^{k_1} \cdots x_M^{k_M} \\ &= \exp \left(\sum_{j=1}^M \beta_{\mathcal{A}_i, \mathcal{A}_j} (x_j - 1) \right). \end{aligned} \quad (28)$$

Third, the generating function of the total number of nodes reachable by following a randomly selected link, which first arrives at a node of \mathcal{A}_i , is defined as $H_1^{\mathcal{A}_i}(x)$, $1 \leq i \leq M$.

We have the self-consistency relations

$$\begin{aligned} H_1^{\mathcal{A}_i}(x) &= x \sum_{k_1, \dots, k_M=0}^{\infty} q_{\mathcal{A}_i}(k_1, \dots, k_M) [H_1^{\mathcal{A}_1}(x)]^{k_1} \cdots [H_1^{\mathcal{A}_M}(x)]^{k_M} \\ &= x F_1^{\mathcal{A}_i}(H_1^{\mathcal{A}_1}(x), \dots, H_1^{\mathcal{A}_M}(x)) \\ &= x \exp \left(\sum_{j=1}^M \beta_{\mathcal{A}_i, \mathcal{A}_j} (H_1^{\mathcal{A}_j}(x) - 1) \right). \end{aligned} \quad (29)$$

An illustration is provided in Fig. 12(a).

Fourth, the generating function of the total number of nodes reachable by following a randomly selected node of \mathcal{A}_i is defined as $H_0^{\mathcal{A}_i}(x)$, $1 \leq i \leq M$, which can be computed as

$$\begin{aligned} H_0^{\mathcal{A}_i}(x) &= x \sum_{k_1, \dots, k_M=0}^{\infty} p_{\mathcal{A}_i}(k_1, \dots, k_M) [H_1^{\mathcal{A}_1}(x)]^{k_1} \cdots [H_1^{\mathcal{A}_M}(x)]^{k_M} \\ &= x F_0^{\mathcal{A}_i}(H_1^{\mathcal{A}_1}(x), \dots, H_1^{\mathcal{A}_M}(x)) \\ &= x \exp \left(\sum_{j=1}^M \beta_{\mathcal{A}_i, \mathcal{A}_j} (H_1^{\mathcal{A}_j}(x) - 1) \right). \end{aligned} \quad (30)$$

An illustration is provided in Fig. 12(b).

Finally, from (30), the average total number of nodes (or the mean component size) reachable from a randomly selected node in \mathcal{A}_i is $\partial_x H_0^{\mathcal{A}_i}(x)|_{x=1}$, $1 \leq i \leq M$. By arranging in a matrix form, we have (25), where (a) follows (30) and (b) follows (29). From (25), we can see that the mean component size blows up when (7) holds. Specifically, the mean component size diverges as $\frac{1}{|\mathbf{Q}|}$ when $|\mathbf{Q}|$ reaches its first zero, where we use $|\mathbf{Q}|$ to denote the determinant in (7).

The preceding analysis can be generalized to the case with arbitrary degree distribution of the form $p_{\mathcal{A}_i}(k_1, k_2, \dots, k_M) = p_{\mathcal{A}_i}(k_1) p_{\mathcal{A}_i}(k_2) \cdots p_{\mathcal{A}_i}(k_M)$, $1 \leq i \leq M$, as in [34], [35]. The percolation condition in (7) becomes (26).

$$\begin{aligned}
\tilde{\beta}_{\mathcal{A}_i, \mathcal{A}_i} &= \int_0^\infty (1 - p_{\mathcal{A}_i}) \lambda_{\mathcal{A}_i} \\
&\quad \times \mathbb{P}_{G_{\mathcal{A}_i, \mathcal{A}_i}, I_{\mathcal{A}_m, \mathcal{A}_i}, I_{\mathcal{B}_n, \mathcal{A}_i}, I_{\mathcal{C}_s, \mathcal{A}_i}} \left(G_{\mathcal{A}_i, \mathcal{A}_i} \geq \frac{(2^{R_{\mathcal{A}_i}} - 1) (\sum_{m=1}^M I_{\mathcal{A}_m, \mathcal{A}_i} + \sum_{n=1}^N I_{\mathcal{B}_n, \mathcal{A}_i} + \sum_{s=1}^S I_{\mathcal{C}_s, \mathcal{A}_i})}{P_{\mathcal{A}_i} r^{-\alpha}} \right) 2\pi r dr \\
&\stackrel{(a)}{=} \int_0^\infty (1 - p_{\mathcal{A}_i}) \lambda_{\mathcal{A}_i} \mathbb{E}_{I_{\mathcal{A}_m, \mathcal{A}_i}, I_{\mathcal{B}_n, \mathcal{A}_i}, I_{\mathcal{C}_s, \mathcal{A}_i}} \left[\int_{-\infty}^\infty \exp \left\{ -t\theta \left(\sum_{m=1}^M I_{\mathcal{A}_m, \mathcal{A}_i} + \sum_{n=1}^N I_{\mathcal{B}_n, \mathcal{A}_i} + \sum_{s=1}^S I_{\mathcal{C}_s, \mathcal{A}_i} \right) \right\} g_{\mathcal{A}_i, \mathcal{A}_i}(t) dt \right] 2\pi r dr \\
&= \int_{-\infty}^\infty g_{\mathcal{A}_i, \mathcal{A}_i}(t) \int_0^\infty (1 - p_{\mathcal{A}_i}) \lambda_{\mathcal{A}_i} \prod_{m=1}^M \mathbb{E}[\exp(-t\theta I_{\mathcal{A}_m, \mathcal{A}_i})] \prod_{n=1}^N \mathbb{E}[\exp(-t\theta I_{\mathcal{B}_n, \mathcal{A}_i})] \prod_{s=1}^S \mathbb{E}[\exp(-t\theta I_{\mathcal{C}_s, \mathcal{A}_i})] 2\pi r dr dt \\
&\stackrel{(b)}{=} \int_{-\infty}^\infty g_{\mathcal{A}_i, \mathcal{A}_i}(t) \int_0^\infty (1 - p_{\mathcal{A}_i}) \lambda_{\mathcal{A}_i} \exp \left\{ - \left(\sum_{m=1}^M p_{\mathcal{A}_m} \lambda_{\mathcal{A}_m} P_{\mathcal{A}_m}^\delta \mathbb{E}[G_{\mathcal{A}_m, \mathcal{A}_i}^\delta] \right. \right. \\
&\quad \left. \left. + \sum_{n=1}^N p_{\mathcal{B}_n} \lambda_{\mathcal{B}_n} P_{\mathcal{B}_n}^\delta \mathbb{E}[G_{\mathcal{B}_n, \mathcal{A}_i}^\delta] + \sum_{s=1}^S \lambda_{\mathcal{C}_s} P_{\mathcal{C}_s}^\delta \mathbb{E}[G_{\mathcal{C}_s, \mathcal{A}_i}^\delta] \right) \pi r^2 (2^{R_{\mathcal{A}_i}} - 1)^\delta P_{\mathcal{A}_i}^{-\delta} \Gamma(1 - \delta) t^\delta \right\} 2\pi r dr dt \\
&= \frac{(1 - p_{\mathcal{A}_i}) \lambda_{\mathcal{A}_i} P_{\mathcal{A}_i}^\delta \int_{-\infty}^\infty g_{\mathcal{A}_i, \mathcal{A}_i}(t) t^{-\delta} dt}{\left(\sum_{m=1}^M p_{\mathcal{A}_m} \lambda_{\mathcal{A}_m} P_{\mathcal{A}_m}^\delta \mathbb{E}[G_{\mathcal{A}_m, \mathcal{A}_i}^\delta] + \sum_{n=1}^N p_{\mathcal{B}_n} \lambda_{\mathcal{B}_n} P_{\mathcal{B}_n}^\delta \mathbb{E}[G_{\mathcal{B}_n, \mathcal{A}_i}^\delta] + \sum_{s=1}^S \lambda_{\mathcal{C}_s} P_{\mathcal{C}_s}^\delta \mathbb{E}[G_{\mathcal{C}_s, \mathcal{A}_i}^\delta] \right) (2^{R_{\mathcal{A}_i}} - 1)^\delta \Gamma(1 - \delta)}. \tag{31}
\end{aligned}$$

APPENDIX C PROOF OF THEOREM 1

From [36], the Laplace transforms of the interference $I_{\mathcal{A}_m, \mathcal{A}_i}$, $I_{\mathcal{B}_n, \mathcal{A}_i}$, and $I_{\mathcal{C}_s, \mathcal{A}_i}$ are

$$\begin{aligned}
\mathbb{E}[e^{-z I_{\mathcal{A}_m, \mathcal{A}_i}}] &= \exp(-p_{\mathcal{A}_m} \lambda_{\mathcal{A}_m} \pi P_{\mathcal{A}_m}^\delta \mathbb{E}[G_{\mathcal{A}_m, \mathcal{A}_i}^\delta] \Gamma(1 - \delta) z^\delta); \\
\mathbb{E}[e^{-z I_{\mathcal{B}_n, \mathcal{A}_i}}] &= \exp(-p_{\mathcal{B}_n} \lambda_{\mathcal{B}_n} \pi P_{\mathcal{B}_n}^\delta \mathbb{E}[G_{\mathcal{B}_n, \mathcal{A}_i}^\delta] \Gamma(1 - \delta) z^\delta); \\
\mathbb{E}[e^{-z I_{\mathcal{C}_s, \mathcal{A}_i}}] &= \exp(-\lambda_{\mathcal{C}_s} \pi P_{\mathcal{C}_s}^\delta \mathbb{E}[G_{\mathcal{C}_s, \mathcal{A}_i}^\delta] \Gamma(1 - \delta) z^\delta). \tag{32}
\end{aligned}$$

Let $\theta \triangleq \frac{2^{R_{\mathcal{A}_i}} - 1}{P_{\mathcal{A}_i} r^{-\alpha}}$, we have (31), where (a) follows by $\mathbb{P}(G_{\mathcal{A}_i, \mathcal{A}_i} \geq z) = \int_{-\infty}^\infty e^{-zt} g_{\mathcal{A}_i, \mathcal{A}_i}(t) dt$ with $z = \theta (\sum_{m=1}^M I_{\mathcal{A}_m, \mathcal{A}_i} + \sum_{n=1}^N I_{\mathcal{B}_n, \mathcal{A}_i} + \sum_{s=1}^S I_{\mathcal{C}_s, \mathcal{A}_i})$, and (b) follows by (32).

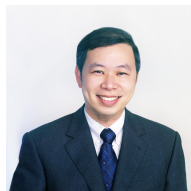
REFERENCES

- [1] I. Akyildiz, W. Lee, M. Vuran, and S. Mohanty, "NeXt generation/dynamic spectrum access/cognitive radio wireless networks: A survey," *Comput. Netw.*, vol. 50, no. 13, pp. 2127–2159, Sept. 2006.
- [2] Y.-C. Liang, K.-C. Chen, G. Y. Li, and P. Mahonen, "Cognitive radio networking and communications: An overview," *IEEE Trans. Veh. Technol.*, vol. 60, no. 7, pp. 3386–3407, Sept. 2011.
- [3] K.-C. Chen, B. K. Cetin, Y.-C. Peng, N. Prasad, J. Wang, and S. Lee, "Routing for cognitive radio networks consisting of opportunistic links," *Wirel. Commun. Mob. Comput.*, vol. 10, no. 4, pp. 451–466, Apr. 2010.
- [4] P. Gupta and P. R. Kumar, "The capacity of wireless networks," *IEEE Trans. Inf. Theory*, vol. 46, no. 2, pp. 388–404, Mar. 2000.
- [5] B. Liu, Z. Liu, and D. Towsley, "On the capacity of hybrid wireless networks," in *Proc. IEEE INFOCOM '03*, Apr. 2003.
- [6] D. M. Shila, Y. Cheng, and T. Anjali, "Throughput and delay analysis of hybrid wireless networks with multi-hop uplinks," in *Proc. IEEE INFOCOM '11*, Apr. 2011.
- [7] C. Wang, X.-Y. Li, C. Jiang, S. Tang, and Y. Liu, "Multicast throughput for hybrid wireless networks under Gaussian channel model," *IEEE Trans. Mobile Comput.*, vol. 10, no. 6, pp. 839–852, June 2011.
- [8] P. Gupta and P. R. Kumar, "Critical power for asymptotic connectivity," in *Proc. IEEE CDC '98*, 1998.
- [9] H. Zhang and J. C. Hou, "Asymptotic critical total power for k-connectivity of wireless networks," *IEEE/ACM Trans. Netw.*, vol. 16, no. 2, pp. 347–358, Apr. 2008.
- [10] P. Santi and D. M. Blough, "The critical transmitting range for connectivity in sparse wireless ad hoc networks," *IEEE Trans. Mobile Comput.*, vol. 2, no. 1, pp. 25–39, Jan. 2003.
- [11] X. Ta, G. Mao, and B. D. O. Anderson, "On the giant component of wireless multihop networks in the presence of shadowing," *IEEE Trans. Veh. Technol.*, vol. 58, no. 9, pp. 5152–5163, Nov. 2009.
- [12] M. Franceschetti and R. Meester, *Random Networks for Communication: From Statistical Physics to Information Systems*. Cambridge University Press, 2008.
- [13] R. Hekmat and P. V. Miegheem, "Connectivity in wireless ad hoc networks with a log-normal radio model," *Mob. Netw. Appl.*, vol. 11, no. 3, pp. 351–360, June 2006.
- [14] D. Miorandi, E. Altman, and G. Alfano, "The impact of channel randomness on coverage and connectivity of ad hoc and sensor networks," *IEEE Trans. Wireless Commun.*, vol. 7, no. 3, pp. 1062–1072, Mar. 2008.
- [15] M. Haenggi, "A geometric interpretation of fading in wireless networks: Theory and applications," *IEEE Trans. Inf. Theory*, vol. 54, no. 12, pp. 5500–5510, Dec. 2008.
- [16] O. Dousse, F. Baccelli, and P. Thiran, "Impact of interferences on connectivity in ad hoc networks," *IEEE/ACM Trans. Netw.*, vol. 13, no. 2, pp. 425–436, Apr. 2005.
- [17] Z. Kong and E. M. Yeh, "Connectivity and latency in large-scale wireless networks with unreliable links," in *Proc. IEEE INFOCOM '08*, Apr. 2008.
- [18] D. Goeckel, B. Liu, D. Towsley, L. Wang, and C. Westphal, "Asymptotic connectivity properties of cooperative wireless ad hoc networks," *IEEE J. Sel. Areas Commun.*, vol. 27, no. 7, pp. 1226–1237, Sept. 2009.
- [19] O. Dousse, P. Thiran, and M. Hasler, "Connectivity in ad-hoc and hybrid networks," in *Proc. IEEE INFOCOM '02*, 2002.
- [20] R. K. Ganti and M. Haenggi, "Single-hop connectivity in interference-limited hybrid wireless networks," in *Proc. IEEE ISIT '07*, 2007.
- [21] C. Yi and W. Wang, "On the connectivity analysis over large-scale hybrid wireless networks," in *Proc. IEEE INFOCOM '10*, Mar. 2010.
- [22] W. Ren, Q. Zhao, and A. Swami, "Connectivity of heterogeneous wireless networks," *IEEE Trans. Inf. Theory*, vol. 57, no. 7, pp. 4315–4332, July 2011.
- [23] P. Wang, I. F. Akyildiz, and A. M. Al-Dhelaan, "Percolation theory based connectivity and latency analysis of cognitive radio ad hoc networks," *Wirel. Netw.*, vol. 17, no. 3, pp. 659–669, Apr. 2011.
- [24] W. C. Ao, S.-M. Cheng, and K.-C. Chen, "Connectivity of multiple cooperative cognitive radio ad hoc networks," *IEEE J. Sel. Areas Commun.*, vol. 30, no. 2, pp. 263–270, Feb. 2012.
- [25] D. Stoyan, W. Kendall, and J. Mecke, *Stochastic Geometry and Its Applications*, 2nd ed. John Wiley and Sons, 1996.
- [26] J. F. C. Kingman, *Poisson Processes*. Oxford University Press, 1993.
- [27] M. E. J. Newman, "The structure and function of complex networks," *SIAM Rev.*, pp. 167–256, 2003.

- [28] M. Franceschetti, L. Booth, M. Cook, R. Meester, and J. Bruck, "Continuum percolation with unreliable and spread out connections," *J. of Statistical Physics*, vol. 118(3/4), pp. 721–734, Feb. 2005.
- [29] J. G. Andrews, F. Baccelli, and R. K. Ganti, "A tractable approach to coverage and rate in cellular networks," *IEEE Trans. Commun.*, vol. 59, no. 11, pp. 3122–3134, Nov. 2011.
- [30] Z. Wang, A. Scaglione, and R. J. Thomas, "Generating statistically correct random topologies for testing smart grid communication and control networks," *IEEE Trans. Smart Grid*, vol. 1, no. 1, pp. 28–39, June 2010.
- [31] R. K. Ganti and M. Haenggi, "Spatial and temporal correlation of the interference in ALOHA ad hoc networks," *IEEE Commun. Lett.*, vol. 13, no. 9, pp. 631–633, Sept. 2009.
- [32] W. C. Ao and K.-C. Chen, "Bounds and exact mean node degree and node isolation probability in interference-limited wireless ad hoc networks with general fading," *IEEE Trans. Veh. Technol.*, vol. 61, no. 5, pp. 2342–2348, June 2012.
- [33] M. E. J. Newman, S. H. Strogatz, and D. J. Watts, "Random graphs with arbitrary degree distributions and their applications," *Phys. Rev. E*, vol. 64, no. 2, p. 026118, July 2001.
- [34] M. E. J. Newman, "Mixing patterns in networks," *Phys. Rev. E*, vol. 67, no. 2, p. 026126, Feb. 2003.
- [35] A. Allard, P.-A. Noël, L. J. Dubé, and B. Pourbohloul, "Heterogeneous bond percolation on multitype networks with an application to epidemic dynamics," *Phys. Rev. E*, vol. 79, p. 036113, Mar. 2009.
- [36] M. Haenggi, J. G. Andrews, F. Baccelli, O. Dousse, and M. Franceschetti, "Stochastic geometry and random graphs for the analysis and design of wireless networks," *IEEE J. Sel. Areas Commun.*, vol. 27, no. 7, pp. 1029–1046, Sept. 2009.



Weng Chon Ao was born in Macau. He received the B.S. degrees in both computer science and physics from National Taiwan University, Taiwan, in 2008, and the M.S. degree in electrical engineering from National Taiwan University, Taiwan, in 2010. From 2010 to 2012, he was a research assistant with Intel-NTU Connected Context Computing Center, Taiwan. He is currently pursuing the Ph.D. degree in electrical engineering at University of Southern California, Los Angeles, USA. His research interests include stochastic modeling and control of communication networks.



Kwang-Cheng Chen (M'89-SM'93-F'07) received the B.S. degree from National Taiwan University, Taipei, Taiwan, in 1983 and the M.S. and Ph.D. degrees from the University of Maryland, College Park, in 1987 and 1989, respectively, all in electrical engineering.

From 1987 to 1998, he was with SSE; COM-SAT; the IBM Thomas J. Watson Research Center, Yorktown Heights, NY; and National Tsing Hua University, Hsinchu, Taiwan, working on mobile communications and networks. He is currently a Distinguished Professor and Deputy Dean, College of Electrical Engineering and Computer Science, National Taiwan University. His research interests include wireless communications and network science.

Dr. Chen has received a number of awards and honors, including the 2011 IEEE ComSoc WTC Recognition Award. He is a coauthor of three IEEE papers that received the 2001 ISI Classic Citation Award, the IEEE ICC 2010 Best Paper Award, and IEEE GLOBECOM 2010 Gold Best Paper.